

# 1 High-resolution Carbon cycling data from 2019 to 2021 measured at six 2 Austrian Long-Term Ecosystem Research sites

3

4 Thomas Dirnböck<sup>1\*</sup>, Michael Bahn<sup>2</sup>, Eugenio Diaz-Pines<sup>3</sup>, Ika Djukic<sup>1</sup>, Michael Englisch<sup>4</sup>, Karl Gartner<sup>4</sup>,  
5 Günther Gollobich<sup>4</sup>, Johannes Ingrisch<sup>2</sup>, Barbara Kitzler<sup>4</sup>, Karl Knaebel<sup>1</sup>, Johannes Kobler<sup>1</sup>, Andreas  
6 Maier<sup>5</sup>, Armin Malli<sup>4</sup>, Ivo Offenthaler<sup>1</sup>, Johannes Peterseil<sup>1</sup>, Gisela Pröll<sup>1</sup>, Sarah Venier<sup>1</sup>, Christoph  
7 Wohner<sup>1</sup>, Sophie Zechmeister-Boltenstern<sup>3</sup>, Anita Zolles<sup>4</sup>, Stephan Glatzel<sup>5</sup>

8

9 <sup>1</sup> Environment Agency Austria, Spittelauer Lände 5, A-1090 Vienna, Austria

10 <sup>2</sup> Department of Ecology, Universität Innsbruck, Innsbruck, Austria; Innrain 52, 6020 Innsbruck

11 <sup>3</sup> Institute of Soil Research, Department of Forest- and Soil Sciences, BOKU University. Peter-Jordan-  
12 Straße 82, 1190 Vienna, Austria

13 <sup>4</sup> Austrian Research Centre for Forests, Seckendorff-Gudent Weg 8, 1131 Vienna, Austria

14 <sup>5</sup> Department of Geography and Regional Research, Faculty of Earth Sciences, Geography and  
15 Astronomy, University of Vienna, Josef-Holaubek-Platz 2, 1090 Vienna, Austria

16 \*corresponding author: Thomas Dirnböck; thomas.dirnboeck@umweltbundesamt.at

17

18 Abstract

19 Seven long-term observation sites have been established in six regions across Austria, covering major  
20 ecosystem types such as forests, grasslands and wetlands across a wide bioclimatic range. The  
21 purpose of these observations is to measure key ecosystem parameters serving as baselines for  
22 assessing the impacts of extreme climate events on the carbon cycle. The data sets collected include  
23 meteorological variables, soil microclimate, CO<sub>2</sub> fluxes and tree stem growth, all recorded at high  
24 temporal resolution (15 – 60 minutes) between 2019 and 2021 (including one year of average  
25 climate conditions and two comparatively dry years). The DOIs of the dataset can be found in the  
26 data availability chapter. The sites will be integrated into the European Research Infrastructure for  
27 Integrated European Long-Term Ecosystem, Critical Zone, and Socio-Ecological Research (eLTER RI).  
28 Subsequently, new data covering the variables presented here will be continuously available through  
29 its data integration portal. This step will allow the data to reach its full potential for research on  
30 drought-related ecosystem carbon cycling.

31

32 1. Introduction

33 Climate change has been affecting ecosystems globally with strong implications for the terrestrial  
34 carbon (C) cycle, which in turn feeds back to the climate system (Heimann and Reichstein, 2008). As  
35 an emerging feature of climate change, extreme climatic events (ECEs) are expected to occur with  
36 increasing frequency and intensity in the coming decades (IPCC, 2021). ECEs are considered to exert  
37 stronger impacts on ecosystems and the services they provide to mankind than gradual changes in  
38 climate (Frank et al., 2015; Reichstein et al., 2013; Grünzweig et al., 2022; Anderegg et al., 2020).  
39 Understanding, predicting and managing extreme climate events and their consequences for  
40 ecosystems and societies will therefore be one of the big challenges in the coming decades. To detect

41 and attribute impacts of ECEs on ecosystem processes and services they need to be evaluated on the  
42 background of the typical interannual range of these processes (Ciais et al., 2005; Bernal et al., 2012;  
43 Fu et al., 2020; Schindlbacher et al., 2012) and analyses of ecosystem resilience to ECEs require a  
44 robust quantification of baselines of ecosystem functioning (Bahn and Ingrisch, 2018; Ingrisch and  
45 Bahn, 2018). For deriving such baselines as well as interannual variability of ecosystem carbon  
46 cycling, coordinated and representative observation networks need to be in place to enable data  
47 retrieval as well as rapid-response scientific campaigns to study after-effects and post-disturbance  
48 trajectories resulting from ECEs (Kulmala, 2018; Mahecha et al., 2017; Mirtl et al., 2018; Dirnböck et  
49 al., 2019; Müller and Bahn, 2022). Datasets obtained through such observation networks are also  
50 essential for benchmarking models (Futter et al., 2023; Baatz et al., 2021; Wu et al., 2018) and for  
51 comparison with ecosystem experiments (Kröel-Dulay et al., 2022).

52 Within a research infrastructure project focusing on ecosystem carbon, nitrogen, and water fluxes  
53 (Long-Term Ecosystem Research for Carbon, Water, and Nitrogen (LTER-CWN, [https://www.lter-  
54 austria.at/cwn/](https://www.lter-austria.at/cwn/)), we equipped seven long-term observation sites in six regions, which are part of the  
55 existing Long-Term Ecological Research Network of Austria (LTER-Austria), with high temporal  
56 resolution (30-60 minutes) C cycle measurements. The sites cover three major ecosystem types  
57 occurring across Austria (forests, managed mountain grassland, wetlands) and most of them are part  
58 of socio-ecological research platforms for transdisciplinary studies (Figure 1). Here, we provide  
59 observational ecosystem response data capturing naturally-occurring ECEs from the first three years  
60 after the onset of the infrastructure, 2019 to 2021. These data sets include meteorological variables,  
61 soil microclimate, CO<sub>2</sub> flux measurements using automated chambers (soil CO<sub>2</sub> efflux) and eddy  
62 covariance techniques (net ecosystem exchange), respectively, and tree stem radial increments and  
63 shrinkage in forested plots.

64

## 65 2. Site descriptions

66 The sites are key research infrastructures for ecosystem-related greenhouse gas observations in  
67 Austria. They include forests (Klausen-Leopoldsdorf and Rosalia in Lower Austria, Zöbelboden in  
68 Upper Austria, and Stubai in Tyrol), mountain grassland (Stubai, Tyrol), and wetlands (Pürgschachen  
69 Moor, Styria and Lake Neusiedl reed belt, Burgenland). This network of sites covers typical forest,  
70 alpine and wetland ecosystems of Central Europe (Figure 1). Furthermore, the sites represent  
71 different geological characteristics, from crystalline rock in the central Alps to the limestone in the  
72 northern Alps to unconsolidated Holocene sediments in lowlands. All sites are part of the Austrian  
73 LTER network and, once officially launched, will be included in the European eLTER research  
74 infrastructure (<https://elter-ri.eu/>). For a detailed description of the sites, we refer to the Dynamic  
75 Ecological Information Management System - Site and dataset registry (DEIMS-SDR) (Table 1).

### 76 2.1. Rosalia Forest Demonstration Centre (Mixed beech forest)

77 The Rosalia Forest Demonstration Centre was settled in 1972, as a cooperation between the BOKU  
78 University, Vienna, Austria, and the Austrian Federal Forests, and has approximately 1000 ha in the  
79 western slopes of the Rosalia Mountains (Rosaliengebirge) in Lower Austria (Figure 1, Table 1). The  
80 forest hosts all major tree species occurring in Austria, i.e. European beech (*Fagus sylvatica* L.),  
81 Norway spruce (*Picea abies* (L.) H.Karst.), Scots pine (*Pinus sylvestris* L.), Larch (*Larix decidua* Mill.),  
82 and Fir (*Abies alba* Mill.). The altitude ranges from 320 to 725 m a.s.l., and mean annual temperature  
83 and mean annual precipitation are 6.5 °C and 796 mm, respectively. Substrate is mainly composed by  
84 crystalline rocks, and soils are predominantly cambisols (Working Group WRB 2015); sporadically in

85 combination with planosols (in plains and moderate slopes), with fluvisols (in valleys) or podzolic  
86 cambisols (steep slopes) (Fürst et al., 2021).

87 The demonstration forest holds several experimental and observation sites distributed along its area,  
88 including water, soil, vegetation and air observations (e.g. Gillespie et al., 2023). A watershed (220  
89 ha) is subject to hydrological observations (Fürst et al., 2021), and the forest is regularly monitored  
90 on permanent plots (Gollob et al., 2020). The meteorological data presented here originates from  
91 three stations located at 385 (Mehlbeerleiten), 500 (Kuhwald) and 640 m a.s.l. (Heuberg). The C cycle  
92 data was measured on a long-term experimental site launched in 2012. The site is located in a pure  
93 mature beech stand at 600 m a.s.l. (47° 42' 26" N; 16° 17' 59" E). It faces north-west, with a slope of  
94 approximately 20 %. This experiment focuses on investigating the effect of changing precipitation  
95 patterns on soil nitrogen fluxes, soil microbial changes, greenhouse gas efflux, and soil water  
96 processes (Leitner et al., 2017; Liu et al., 2019; Schwen et al., 2015; Gillespie et al., 2024). Monitoring  
97 is performed on control and on manipulated plots. The data from both natural and manipulated plots  
98 is published with this paper. Manipulation involves the use of rain-out-shelters (for simulating  
99 drought periods of different length) and of an irrigation system (for recreating rainfall events of  
100 different intensity). The monitoring infrastructure involves the measurements of greenhouse gases  
101 (GHG) (N<sub>2</sub>O, CH<sub>4</sub> and CO<sub>2</sub>) fluxes, soil nutrients (suction cups) and microclimate parameters.

## 102 2.2. Klausen-Leopoldsdorf (Beech forest)

103 The site, Klausen-Leopoldsdorf, is located about 40 km south-west of Vienna on a NNE-facing slope  
104 and was founded in the 1990s as one of Austria's site contributing to the International Co-operative  
105 Programme on Assessment and Monitoring of Air Pollution Effects on Forests (ICP Forests) (Neumann  
106 and Starlinger, 2001). The site is divided into four different sub-areas within a small catchment: 1)  
107 the ICP Forests site, 2) a weather station, located 2.7 km from the ICP Forests intensive plots at 398  
108 m a.s.l., 3) a catchment runoff weir (475 m a.s.l.), and 4) the LTER-CWN measurement plot (520 m  
109 a.s.l.), where the C-cycle data presented here was measured (Figure 1, Table 1). The forest within the  
110 measurement plot is a pure beech (*Fagus sylvatica* L.) stand. The mean annual temperature is 8°C,  
111 mean annual precipitation is 801 mm (2010-2022). The geological substrate is sandstone, the soil  
112 type is mainly stagnic cambisol/dystric cambisol (Working Group WRB 2015). Instruments installed  
113 on the LTER-CWN measurement area include a sap flow and dendrometer measurement system on  
114 10 trees, 12 GHG automated measurement chambers for CO<sub>2</sub> respiration, soil moisture and soil  
115 temperature sensors in different soil depths (5 – 30 cm).

116 In addition to the data presented here, many other data sets are available. Soil GHG fluxes (manual  
117 sampling) were measured starting in the year 2001 (Kitzler et al., 2006). On the ICP Forests site,  
118 instruments for long-term monitoring (since 1996) such as soil moisture, air temperature and relative  
119 humidity, soil temperature, soil solution with suction cups, throughfall deposition, litterfall traps,  
120 stemflow, and manual and automatic dendrometers are installed and the data is available under  
121 <https://bfw.ac.at/lims/level2.daten> or via the ICP Forests Program Centre.

## 122 2.3. Lake Neusiedl (reed belt)

123 The measurement site is located in the eastern reed belt of the lake and as such inside the National  
124 Park Lake Neusiedl - Seewinkel (Figure 1, Table 1). The region (average altitude: 120 m.a.s.l.) is  
125 characterized by a (sub)-continental Pannonian climate with a mean annual precipitation of 576 mm  
126 (2013-2022). The reed belt is a dynamic ecosystem consisting of a mosaic of reed stocks (*Phragmites*  
127 *australis* (Cav.) Trin. ex Steud.), sediment and open water areas. Increasing dry periods and thus  
128 successive drying of the reed belt since 2018 have led to an increase in reed stocks within the belt, as  
129 well as an increase in sediment areas and a strong decline in open water areas, according to a 2021

130 study that investigated the spatial and temporal variations within the reed ecosystem at Lake  
131 Neusiedl (Buchsteiner et al., 2023). Processes driving CH<sub>4</sub> emissions from the reed belt have recently  
132 been investigated in detail (Baur et al., 2024).

133 The data presented here stems from devices permanently installed on site. They include an eddy  
134 covariance tower for CO<sub>2</sub>, CH<sub>4</sub> and water vapor fluxes and relevant accompanying meteorological  
135 parameters as well as soil heat flux, soil moisture, and soil temperature sensors.

#### 136 2.4. Pürgschachen Moor (peat bog)

137 The Pürgschachen Moor is located on the bottom of the Styrian Enns valley at an altitude of 632 m  
138 a.s.l. (Figure 1, Table 1). It is a pine peat bog with an extent of about 62 ha. Thus, it is the largest (to a  
139 large part) intact valley peat bog in Austria with a closed peat moss cover and a good example of the  
140 formerly widely distributed peatlands of inner-alpine valleys of the European Alps. The mean average  
141 temperature is 8.2 °C and mean annual precipitation is 1233 mm (2013-2022). The typical vegetation  
142 of the peat bog is constituted of three associations of plants *Pino mugo-Sphagnetum magellanici*  
143 (pine peat bog association), *Sphagnetum magellanici* (coloured bog moss association), and *Caricetum*  
144 *limosae* (bog sedge association), depending on the prevailing hydrological site conditions. The  
145 current mean water table depth is about 14 cm below soil surface at the central peat bog area. Peat  
146 decomposition and related CO<sub>2</sub> and CH<sub>4</sub> fluxes were subject of a series of research studies (Drollinger  
147 et al., 2019; Knierzinger et al., 2020; Müller et al., 2022; Glatzel et al., 2023).

148 The data presented here stems from devices permanently installed roughly in the center of the peat  
149 bog. They include an eddy covariance tower for CO<sub>2</sub>, CH<sub>4</sub> and water vapor fluxes and relevant  
150 accompanying meteorological parameters as well as soil heat flux, soil moisture, and soil  
151 temperature sensors.

#### 152 2.5. Stubai (subalpine hay meadow, Larch and Spruce forest)

153 The two observation plots used in this study are part of the LTER Site Stubai (Table 1), which is  
154 located in the Stubai Alps in Tyrol, Austria (Figure 1). Research at the study site was established in  
155 1993. The two observation plots are a mountain grassland and a subalpine forest at an alpine pasture  
156 area called "Kaserstattalm". The underlying rock is siliceous and calcareous. The average air  
157 temperature is about 3°C and the precipitation approx. 1100 mm. About 35% of the annual  
158 precipitation occurs as snow during winter months.

159 The grassland site is located at an altitude of 1810 -1850 m a.s.l on a south-east facing slope with an  
160 inclination of ca. 20°. The site is an extensively managed meadow that is harvested once a year in  
161 early August and grazed lightly in late summer. The soil is a dystric cambisol (Working Group WRB  
162 2015). The vegetation type is a *Trisetetum flavescens* and consists of perennials grasses and forbs  
163 dominated by *Agrostis capillaris* L., *Festuca rubra* L., *Anthoxanthum odoratum* L., *Ranunculus*  
164 *montanus* Willd., *Leontodon hispidus* L., *Trifolium repens* L. and *T. pratense* L. (Bahn et al., 2009;  
165 Schmitt et al., 2010).

166 The forested observation plot is located close to the tree line at 1960 m a.s.l. on a slope with an  
167 inclination of 20-35°. It is dominated by the two common tree species European larch (*Larix decidua*  
168 Mill.) and Norway spruce (*Picea abies* (L.) H.Karst.). In former years, the plot was a pasture and it was  
169 reforested in the 1980s (Oberleitner et al., 2022).

170 Both observation plots are equipped with micrometeorological stations, soil environment monitoring  
171 (soil moisture, soil temperature), and soil CO<sub>2</sub> devices. At both observation plots, we measured soil  
172 CO<sub>2</sub> fluxes with automated chambers during the summer. The forest plot is additionally equipped  
173 with tree dendrometers and tree sapflow sensors. In the grassland, land use and drought related

174 carbon cycle research was carried out over the last two decades (Fuchslueger et al., 2014; Hasibeder  
175 et al., 2015; Ingrisch et al., 2020; Ingrisch et al., 2018). Research using the forest plot started only  
176 recently (Oberleitner et al., 2022).

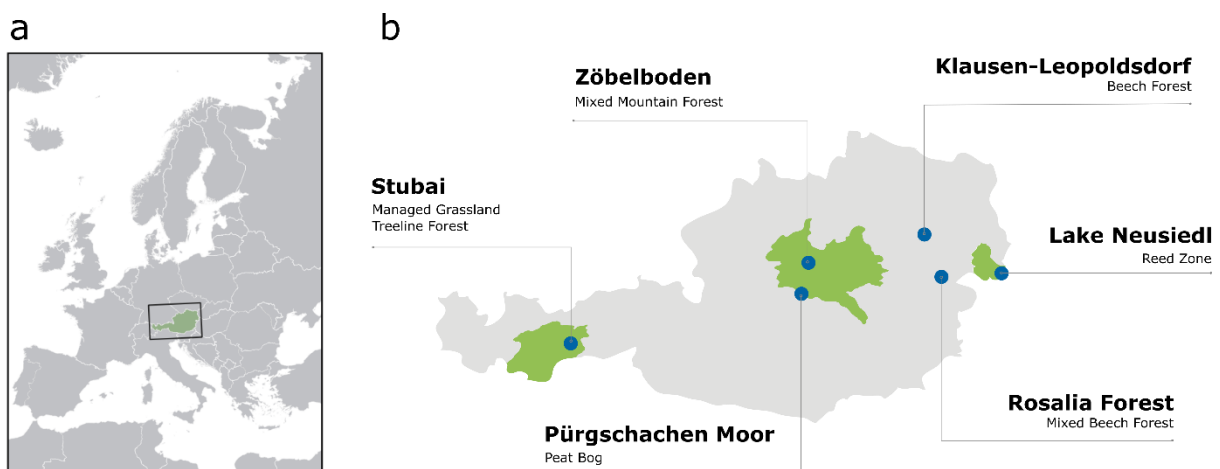
## 177 2.6. Zöbelboden (mixed Beech forest)

178 The site LTER Zöbelboden is located in the National Park Kalkalpen in the Northern Limestone Alps,  
179 Austria (Figure 1). The measurements were established in 1992 as part of the International Cooperative  
180 Programme on Integrated Monitoring of Air Pollution Effects on Ecosystems (ICP IM) covering a 90 ha  
181 catchment with an elevation range of 550 to 956 m a.s.l. (Table 1). The main underlying rock type is  
182 Norian dolomite (*Hauptdolomit*), partly overlain by limestone (*Plattenkalk*). According to long-term  
183 meteorological measurements (1993-2022), mean annual air temperature and precipitation are 8.2 °C  
184 and 1645 mm, respectively. Maximum precipitation occurs in summer and snowfall usually between  
185 December and April.

186 The data presented here was measured at the Intensive Plot II situated on a steep (36° on average)  
187 north-westerly exposed slope at 880 m a.s.l. The soils of the plot are lithic and rendzic leptosols  
188 (Working Group WRB 2015). The plot is dominated by beech (*Fagus sylvatica* L.) with intermixed  
189 sycamore (*Acer pseudoplatanus* L.), European ash (*Fraxinus excelsior* L.) and spruce (*Picea abies* (L.)  
190 H.Karst.). Since the year 1995, this plot is equipped with a number of field measurement devices for  
191 long-term monitoring (throughfall deposition, litter fall traps, lysimeters, soil moisture and  
192 temperature sensors, manual dendrometers) and supplemented by other monitoring activities (tree  
193 inventory, needle and leave chemistry, soil chemistry, etc.; see e.g. Leitner et al., 2020; Kobler et al.,  
194 2019; Dirnböck et al., 2016; Dirnböck et al., 2020). Drought-impacts on carbon allocation in the  
195 forests of the catchment is currently one of the research foci for which long-term observation data  
196 exists (see e.g. Hartl-Meier et al., 2014) as well as experimental plots with rainout shelters.

197 The instruments and data included here are soil respiration automated chambers, soil water  
198 potential and temperature sensors as well as automated dendrometers. The meteorological data  
199 stems from a station in close proximity at the plateau at 890 m a.s.l.. The site is also equipped with  
200 an Eddy covariance tower, but this data will be published elsewhere.

201



202

203 *Figure 1.* Location of sites in Europe (a) and Austria (b). Blue dots indicate the sites; green areas are long-term socio-  
204 ecological research platforms (LTSEr) (from left to right: LTSEr Tyrolian Alps, LTSEr Eisenwurzen, and LTSEr Lake Neusiedl)  
205 within the LTER Austria network. For site information concerning altitude and climate see Table 1.

206  
207

Table 1. Ecosystem type, altitude, climate and metadata links of the sites and observation plots. Geographic boundaries, linked data sets, etc. can be found in the site and dataset registry system DEIMS-SDR.

| Site                                      | Ecosystem type        | Altitude (m a.s.l.) | Annual temperature (°C) | Annual precipitation (mm) | Site and observation plot             | DEIMS.ID   |
|---|-----------------------|---------------------|-------------------------|---------------------------|---------------------------------------|--|
| Rosalia Forest Demonstration Centre (ROS) | Mixed beech forest    | 600                 | 6.5                     | 796                       | Site                                  | <a href="https://deims.org/77c127c4-2ebe-453b-b5af-61858ff02e31">https://deims.org/77c127c4-2ebe-453b-b5af-61858ff02e31</a>  |
|   |                       |                     |                         |                           | Heuberg Meteorological Station        | <a href="https://deims.org/locations/44854b32-64c3-4c9d-9aec-9b0b74f8ac70">https://deims.org/locations/44854b32-64c3-4c9d-9aec-9b0b74f8ac70</a>  |
|   |                       |                     |                         |                           | Kuhwald Meteorological Station        | <a href="https://deims.org/locations/1225d57e-02da-47fd-9760-ab39d64999ef">https://deims.org/locations/1225d57e-02da-47fd-9760-ab39d64999ef</a>  |
|   |                       |                     |                         |                           | Mehlbeerleiten Meteorological Station | <a href="https://deims.org/locations/0becf0ce-98d7-4f64-a074-f89046083e5e">https://deims.org/locations/0becf0ce-98d7-4f64-a074-f89046083e5e</a>  |
|   |                       |                     |                         |                           | Experimental Station                  | <a href="https://deims.org/locations/b7008603-fca2-452f-9b3d-aad30cdafc7a">https://deims.org/locations/b7008603-fca2-452f-9b3d-aad30cdafc7a</a>  |
| Klausen-Leopoldsdorf (KLL)                | Beech forest          | 520                 | 8                       | 801                       | Site<br>Measuring station             | <a href="https://deims.org/bb472a51-f85f-4de0-8358-f21ecbe2a102">https://deims.org/bb472a51-f85f-4de0-8358-f21ecbe2a102</a><br><a href="https://deims.org/locations/d5cba3ce-7489-46d1-8d97-61641ffb5758">https://deims.org/locations/d5cba3ce-7489-46d1-8d97-61641ffb5758</a> |
| Lake Neusiedl (NSS)                       | reed zone             | 120                 | 11.5                    | 576                       | Same as site                          | <a href="https://deims.org/locations/4234987b-9031-4332-9bdd-f869d503ac51">https://deims.org/locations/4234987b-9031-4332-9bdd-f869d503ac51</a>  |
| Pürgschachen Moor (PUE)                   | peat bog              | 632                 | 8.2                     | 1233                      | Same as site                          | <a href="https://deims.org/locations/ab2d021b-f318-487a-a85b-ab34566e4c02">https://deims.org/locations/ab2d021b-f318-487a-a85b-ab34566e4c02</a>  |
| Stubai (KAS)                              | grassland             | 1830                | 3                       | 1100                      | Site<br>Kaserstattalm meadow          | <a href="https://deims.org/324f92a3-5940-4790-9738-5aa21992511c">https://deims.org/324f92a3-5940-4790-9738-5aa21992511c</a><br><a href="https://deims.org/locations/cf7843b7-32d6-44e9-ba82-9a8d915036a7">https://deims.org/locations/cf7843b7-32d6-44e9-ba82-9a8d915036a7</a> |
|   | Treeline forest       | 1960                | 3                       | 1100                      | Kaserstattalm forest                  | <a href="https://deims.org/locations/af2afdad-d6fb-4580-b6e3-be7d07b56f8e">https://deims.org/locations/af2afdad-d6fb-4580-b6e3-be7d07b56f8e</a>  |
| Zöbelboden (ZOE)                          | Mixed mountain forest | 880                 | 8.2                     | 1645                      | Site<br>Intensive Plot II             | <a href="https://deims.org/8eda49e9-1f4e-4f3e-b58e-e0bb25dc32a6">https://deims.org/8eda49e9-1f4e-4f3e-b58e-e0bb25dc32a6</a><br><a href="https://deims.org/locations/bc96a499-1b20-4da8-be2d-17306d64b788">https://deims.org/locations/bc96a499-1b20-4da8-be2d-17306d64b788</a> |

208

209 3. Dataset description, measuring methods, QA/QC

210 We followed routine quality assurance (QA) and quality control (QC) procedures to ensure  
211 functionality of the sensors and data quality comprising remote function control, on-site check of  
212 sensors and cables, regular sensor calibration, data checks through different quality assurance  
213 procedures (e.g. exceedance of thresholds, outlier detection, deviations from other measurements),  
214 and data quality flagging.

215 3.1. Meteorology, soil temperature and soil moisture

216 All meteorological stations are located within the boundaries of the respective sites except for  
217 Klausen-Leopoldsdorf, where the station is at a distance of 2.7 km from the site. Meteorological  
218 measurements in the wetland sites were implemented next to the Eddy Covariance tower. In  
219 addition to the routine data checks, we compared the measurements with nearby stations where  
220 appropriate. Meteorological measurements were detected in a one-minute-interval and averaged  
221 over half-hour periods while rain data was summed. The measurements include air temperature,  
222 precipitation, relative humidity, wind speed and direction, air pressure, and several radiation  
223 variables (at least global radiation, but also short- and longwave radiation, photosynthetic active  
224 radiation, etc.).

225 *Table 2. Meteorological parameters measured at the six sites during 2019-2021. Availability is indicated using grey boxes.*  
226 *For parameter names we refer to the thesaurus at <http://vocabs.lter-europe.net/EnvThes/>*

227

Meteorological parameters

|                                     | KAS | KLL | NSS | PUE | ROS | ZOE |
|-------------------------------------|-----|-----|-----|-----|-----|-----|
| air relative humidity               |     |     |     |     |     |     |
| air pressure                        |     |     |     |     |     |     |
| air temperature                     |     |     |     |     |     |     |
| precipitation amount                |     |     |     |     |     |     |
| global radiation irradiance         |     |     |     |     |     |     |
| net radiation irradiance            |     |     |     |     |     |     |
| photosynthetically active radiation |     |     |     |     |     |     |
| sunshine duration                   |     |     |     |     |     |     |
| wind direction                      |     |     |     |     |     |     |
| wind speed                          |     |     |     |     |     |     |

228

229 We used different types of soil temperature and soil moisture or soil water potential sensors,  
230 respectively (PT100 or thermoelements for soil temperature, TDR or FDR-sensors for soil moisture, and  
231 soil water potential sensors). Before we buried the soil temperature or soil moisture and soil water  
232 potential sensors into the soil, they had been calibrated or at least tested for consistency. Mostly, we  
233 used gravimetric samples to calibrate the TDR and FDR soil moisture sensors. At Zöbelboden, where  
234 stony, organic rich soils occur, we corrected the TDR values using water potential sensor data installed  
235 in the same soil profiles together with soil water retention functions derived from undisturbed soil  
236 cores. In addition to the regular QC procedures, we checked the data for consistency of the values  
237 across sensors (e.g. along the soil profiles) and compared them with other measurements (air  
238 temperature and precipitation). Half-hourly to hourly values are presented.

239 3.2. Carbon fluxes

240 3.2.1. Soil CO<sub>2</sub> efflux

241 We measured soil CO<sub>2</sub> efflux at five of the seven observation plots. The automated soil CO<sub>2</sub> respiration  
 242 measurement systems are capable of operating autonomously during the snow-free periods The  
 243 measurement chambers and measurement systems collected air from the chamber headspace  
 244 continuously to determine the exchange of CO<sub>2</sub> between soil and atmosphere at the observation plots.  
 245 In all sites, we used non-steady state, non through-flow chambers (Pumpanen et al., 2004). The  
 246 chambers at each site measured consecutively every half-hour to hour. In addition to the automated  
 247 systems, manual flux measurements were also performed which served to validate the automated  
 248 measurement systems. Table 3 provides detailed information on the measurement systems used at  
 249 the sites.

250 Two different automated chamber systems were used: a LI-COR System and custom-made chambers  
 251 in combination with LI-COR trace gas analysers (Table 3). The custom-made soil chambers are  
 252 equipped with a fan and a thermometer. The controlling unit and the gas analyzer (either a CH<sub>4</sub>/CO<sub>2</sub>  
 253 LI-COR 7810, a LI-COR 840, or a LI-COR 8100A, LI-COR Biosciences, USA) are located in already  
 254 existing measurement containers. Remote access to the devices allows for checking plausibility of the  
 255 data and chamber leakage in real time. We visited the instruments at weekly to monthly intervals,  
 256 with maintenance and supervision works including a check of the tightness of the gas lines,  
 257 connections and chamber lids, the correct closing and opening of the chambers and the functioning  
 258 of ventilation fans inside the chambers, ingrowth of plants, and the gas analyser. The gas analysers  
 259 were calibrated once a year in the laboratory with calibration gases. We de-installed and serviced the  
 260 chambers during winter but frames stayed permanently on site to avoid disturbance of the soil.

261 At Klausen-Leopoldsdorf, the gas fluxes of readings were determined using the R package "gasfluxes"  
 262 (Fuss, 2020). At Rosalia, a custom-made Python script was used. Zöbelboden and Kaserstattalm  
 263 process the data with SoilFlux Pro Software (LI-COR Biosciences, 2019). We used the R<sup>2</sup> of the fitted  
 264 empirical models to select valid data. We refer to Table 3 and the metadata published with the data  
 265 for the detailed specifications.

266 *Table 3. Specifications of the different soil CO<sub>2</sub> flux systems following the standard of (Bond-Lamberty et al., 2021).*

| Field Name      | Description                         | Unit            | Klausen-<br>Leopoldsdorf | Stubai<br>grassland  | Rosalia                | Zöbelboden           |
|-----------------|-------------------------------------|-----------------|--------------------------|----------------------|------------------------|----------------------|
| System          |                                     |                 | auto                     | Auto                 | auto                   | auto                 |
| GHG<br>chambers |                                     |                 | Custom-made<br>(n=12)    | LI-8100-104<br>(n=4) | Custom-<br>made (n=12) | LI-8100-104<br>(n=6) |
| INSTRUMENT      | Measurement<br>instrument model     |                 | LI-COR LI-7810           | LI-8100A             | LI-840                 | LI-8100A             |
| MSMT_VAR        | Type of flux<br>measured            |                 | Soil respiration (Rs)    |                      |                        |                      |
| AREA            | Soil surface<br>measurement<br>area | cm <sup>2</sup> | 2500                     | 317.8                | 2500                   | 317.8                |
| VOLUME          | Volume of<br>measurement<br>chamber | cm <sup>3</sup> | 37500                    | 4076.1               | 37500                  | 4076.1               |
| V/A             | Volume/Area ratio                   | cm              | 15                       | 12.83                | 15                     | 12.83                |



|                     |   |                     |   |                        |                           |                        |
|---------------------|---|---------------------|---|------------------------|---------------------------|------------------------|
| COLLAR_DEPTH        | Depth of collar insertion   | cm                  | 5   | 2                      | 10                        | 2                      |
| OPAQUE              | Opaque chamber  |                     | no  | Yes                    | no                        | yes                    |
| chamber system      | static chamber - closed or open   |                     | non-steady state, non through-flow chambers |                        |                           |                        |
| closing time        | closing time of chamber (=time used for flux calculation)                   | sec                 | 175   | depending on year      | 1620                      | 210                    |
| PLANTS_REMOVED      | Plants removed from inside the collar                                       |                     | no, but hardly any                          | Yes                    | no, but hardly any        | no plants              |
| flow_rate           | sample flow rate through tubing   | l min <sup>-1</sup> | 1   | 1 to 2                 | 0.25                      | 1.7                    |
| FAN                 | Mixing fan in chamber?  |                     | yes   | No                     | yes                       | no                     |
| CRVFIT_CO2          | Flux computation method ("Lin" or "Exp" for linear and exponential, others) |                     | linear                                      | automated <sup>1</sup> | Lin/HMR <sup>2</sup>      | Automated <sup>1</sup> |
| R2_CO2              | R <sup>2</sup> of flux computation  | fraction            | 0.90  | 0.95                   | 0.95                      | 0.99                   |
| Calculation of flux |   |                     | R Package gasfluxes                         | LI-COR Soilflux Pro    | custom-made python script | LI-COR Soilflux Pro    |

<sup>1</sup> "Exp" in the data indicates that the exponential fit was better than the linear fit (Exp\_SSN<Lin\_SSN). "Lin" indicates that the linear fit was better after the maximum number of iterations; the non-linear coefficients have therefore been derived from the linear fit.

<sup>2</sup> Hutchinson and Mosier (1981)

### 267 3.2.2. Eddy Covariance measurements at wetland sites

268 In both wetland sites, the Pürgschachen Moor and Lake Neusiedl, fully equipped Eddy-Covariance  
269 systems are in place. Wind speed and direction were measured using a three-axis ultrasonic  
270 anemometer (WindMaster Pro, Gill Instruments, Lymington, UK). CO<sub>2</sub> and H<sub>2</sub>O mixing ratios were  
271 measured using the closed-path infrared gas analyser LI-7200 while CH<sub>4</sub> was detected with the open  
272 path gas analyser LI-7700 (both LI-COR Inc, Lincoln, USA). The measurements were performed with a  
273 sampling rate of 10 Hz. We installed the devices at a vegetation dependent height, 3.05 m above  
274 ground in the Pürgschachen Moor and in the reed belt of Lake Neusiedl 8.6 m, respectively. The Eddy  
275 Covariance devices were checked daily via remote access, calibrated once a year in the lab, and  
276 monthly in the field.

277 The EC data contains half-hour eddy covariance flux measurements for CO<sub>2</sub>, CH<sub>4</sub> and water vapor. We  
278 calculated the fluxes with the EddyPro<sup>®</sup> Software package in the Express mode with default settings  
279 (double rotation, block averaging, covariance maximization, etc.) as part of the SmartFlux<sup>®</sup> 2 System,  
280 providing fully corrected and valid fluxes with quality flags ranging from 0-2. The final flags are based  
281 on a combination of partial flags accounting for steady state and turbulent conditions. Only fluxes

282 flagged with 0 (best quality fluxes) or 1 (fluxes suitable for general analysis such as annual budgets)  
 283 are shown in the data. Gaps in the data-set result from missing micro-meteorological conditions,  
 284 from data cleaning due to the quality flags or from power breakdowns.

### 285 3.3. Radial tree stem growth at forest sites

286 Zöbelboden, Klausen-Leopoldsdorf, Rosalia used the DR26 sensor (EMS, Brno, Czech Republic), Stubai  
 287 used Ecomatic DC2 (Germany) for registering the radial stem increment in a 15 minutes to 30 minutes  
 288 interval. Maintenance involved avoiding any shift of the sensor during the operation. Concerning data  
 289 quality and control methods the Mini32 software (EMS, Brno, Czech Republic), includes graphical  
 290 features to process the measured stem increment data. Data processing comprises outlier detection  
 291 by visual assessment based on expert knowledge. Ecomatic raw data was treated with custom-made  
 292 R scripts. In both cases, unrealistic values beyond the slowly increasing linear growth rates were  
 293 visually assessed and deleted.

## 294 4. Data file structure

295 We used the eLTER Data specification, which is available on Zenodo  
 296 ([www.doi.org/10.5281/zenodo.6373409](http://www.doi.org/10.5281/zenodo.6373409)). Apart from the data files, the measurement locations  
 297 (Station files) and the sensors (methods) are included.

298

## 299 5. Data validation

300 *Table 4. Comparison between long-term (1980-2010) meteorological drought (SPEI - Standardized Precipitation*  
 301 *Evapotranspiration Index) and the measurement years during the growing season (May-September). Significant differences*  
 302 *between these years and the long-term averages are shown: \*\*\* p<0.001; \*\* p<0.005; \* p<0.01 according to a Mann-*  
 303 *Whitney U Test. SPEI was calculated using a 30 days window in a daily resolution using gridded data:*  
 304 *<https://data.hub.geosphere.at/dataset/winfore-v2-1d-1km> (Haslinger & Bartsch, 2016). Negative values indicate dry years.*

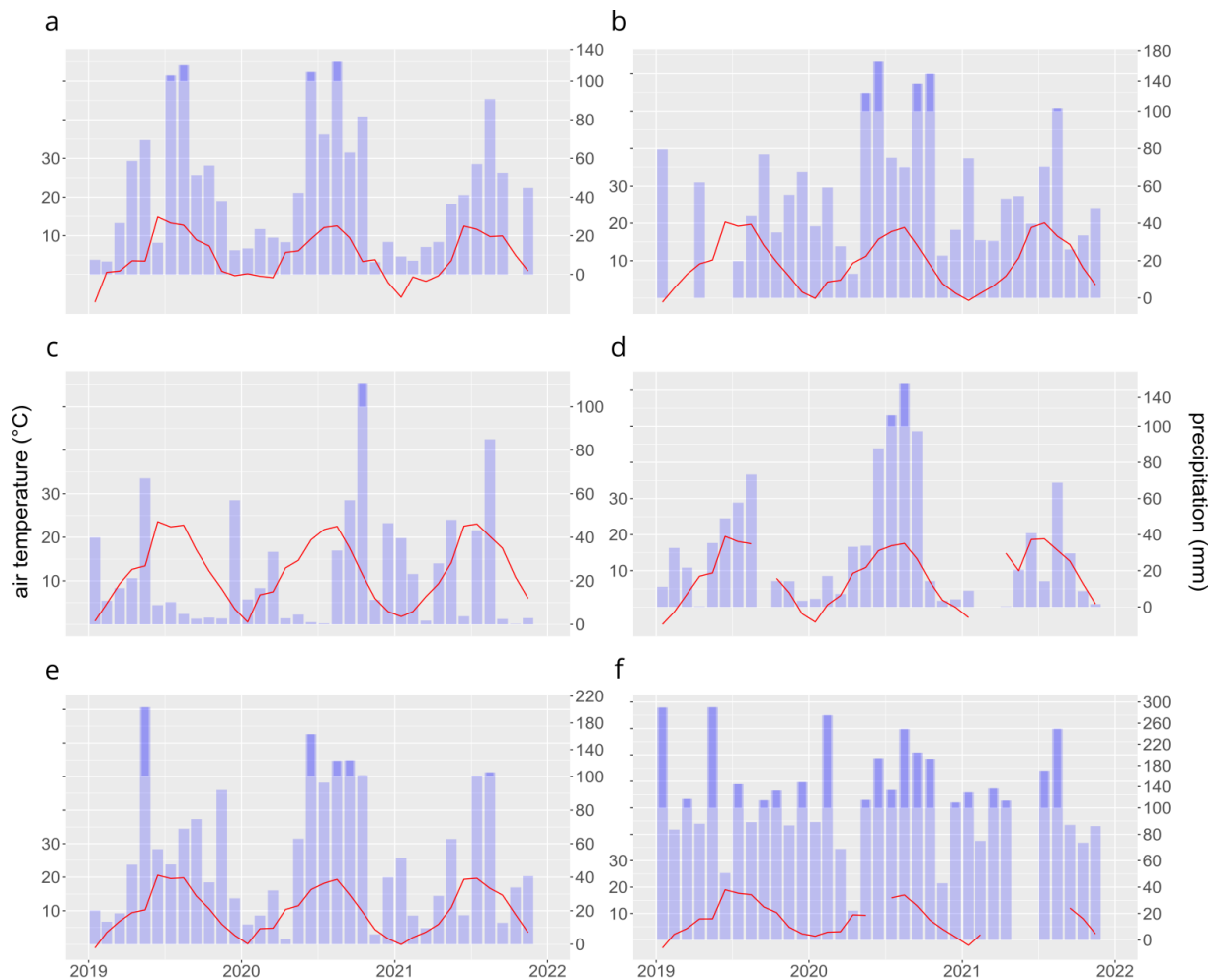
| Site Code | 1980-2010  | 2019          | 2020         | 2021        |
|-----------|------------|---------------|--------------|-------------|
| ZOE       | -0.05±0.94 | -0.49±1.22*** | 0.42±0.69*** | -0.02±1.39  |
| KLL       | -0.01±0.99 | -0.23±1.22    | 0.39±0.86*** | -0.02±1.24  |
| KAS       | -0.05±0.97 | -0.1±1.17     | -0.12±0.78   | 0.23±1.07** |
| PUE       | -0.02±0.94 | -0.54±1.26*** | 0.17±0.59**  | -0.12±1.2   |
| NSS       | -0.01±1    | -0.22±1.13*   | 0.2±0.87**   | -0.2±1.34   |
| ROS       | -0.03±0.98 | -0.34±1.01*** | 0.17±0.83    | -0.28±1.08  |

305

306 We used gridded SPEI (Standardized Precipitation Evapotranspiration Index) from the Austrian  
 307 Meteorological Service (<https://data.hub.geosphere.at/dataset/winfore-v2-1d-1km>; Haslinger &  
 308 Bartsch (2016)) to compare the long-term average water availability during the growing season  
 309 (1980-2010; May to September) with those occurring in the measurement years (Table 4). The  
 310 advantage of the SPEI is that it accounts for precipitation and temperature via evapotranspiration  
 311 and integrates over a given temporal window (we used 30 days) (Vicente-Serrano et al. 2010). Note,  
 312 that gridded SPEI data set is based on meteorological data for the period 1960 to 2021. Accordingly,  
 313 the 2021 was closest to the long-term average, the year 2020 was a particularly wet year, and the  
 314 year 2019 was drier than the average. However, there were differences between the sites:  
 315 particularly the mountain station in the Tyrolian Alps (KAS) did not experience significant deviations  
 316 in SPEI as compared to the long-term average apart from a wet growing season in 2021. The SPEI at  
 317 the site in the Viennese Forest (KLL) does not indicate that in 2019, the growth period was  
 318 particularly dry.

319 The monthly precipitation and temperature patterns are shown in Figure 2, and soil water content  
 320 and soil temperatures in Figure 3 and Figure 5. Differences in the seasonal precipitation patterns  
 321 between the measurement years vary a lot between sites. In sum, lower precipitation occurred in  
 322 2019 and 2021 than in 2020 in all sites. The mean annual temperature maxima (90 percentile) were  
 323 between 0.3 °C (KAS) and 2.3 °C (ZOE) higher in the year 2019 than in 2020. These differences were  
 324 lower when comparing the year 2021 with 2019 ( $\leq 0.6$  °C). In accordance with SPEI, precipitation and  
 325 temperature, soil water content showed the lowest values during the years 2019 followed by the  
 326 year 2021, and soil temperature were higher during these years (Figure 3Figure 4).

327



328

329 *Figure 2.* Monthly mean air temperature (red line) and monthly precipitation sums (blue bars; different scale > 100 mm) at  
 330 Stubai-Kaserstattalm (a), Klausen-Leopoldsdorf (b), Lake Neusiedl(c), Pürgschachen Moor (d), Rosalia (e), and Zöbelboden  
 331 (f).

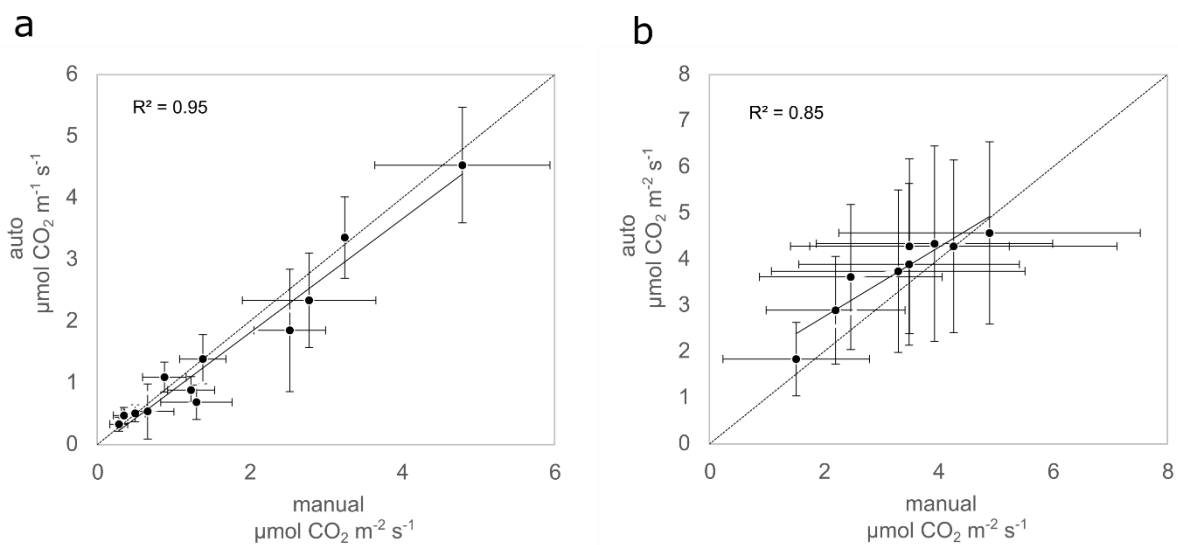
332 We measured soil CO<sub>2</sub> respiration at four sites (Figure 4). The complexity of automated chamber  
 333 measurements resulted in some data gaps: at KAS and ROS during the years 2019 and 2021  
 334 respectively; at KLL and ZOE, the respiration data covers most of the snow-free period (see Table 2).

335 At Klausen-Leopoldsdorf (KLL) and Zöbelboden (ZOE), we compared the automatically measured soil  
 336 CO<sub>2</sub> flux rates with manual measurements. For both sites, we used a portable infrared gas analyzer  
 337 (EGM-4) connected to a manual soil respiration chamber (SRC) (PP Systems International Inc.,  
 338 Amesbury, MA, USA). The two measurement sites were equipped with permanently installed collars  
 339 (KLL: randomly distributed within the site in immediate vicinity of the automated chambers (n = 12);  
 340 area = 284 cm<sup>2</sup> and 2 cm insertion depth; Zöbelboden: regular grid covering the entire plot (n = 30),

341 area = 78 cm<sup>2</sup> and 1.5 cm insertion depth). The chamber closure time was 60 and 100 seconds in KLL  
342 and ZOE, respectively. Manual measurements took place in monthly intervals from Oct. 2019-Jun.  
343 2020 at Klausen-Leopoldsdorf and from Jun. 2019 until Oct. 2019 (monthly interval) and in July 2020  
344 (diurnal variation) at ZOE. Soil respiration (Rs) was calculated automatically by fitting a linear (KLL) or  
345 quadratic function (ZOE; quadratic fit for flow rates > 0.2 ppm s<sup>-1</sup>, otherwise a linear fit was used) to  
346 the increasing CO<sub>2</sub> headspace concentration.

347 The mean CO<sub>2</sub> fluxes of the automated chambers correlated well with the manually measured fluxes  
348 during the measurement campaigns (Figure 3). At KLL, the R<sup>2</sup> was 0.95 (p-value < 0.05, t-test), at ZOE  
349 it was 0.85 (p-value < 0.05, t-test). In both sites, neither the intercept nor the slope was significantly  
350 different from 0 (p-value > 0.2, t-test) and 1 (p-value > 0.49, t-test), respectively. At ZOE, the spatial  
351 flux variation was much higher than at KLL (Figure 3A and 3B). This reflects the heterogeneity of the  
352 soil conditions (shallow rendzic leptosols with interspersed fine-scale patches of deeper soils), the  
353 canopy gaps (with lower root density), and the uneven distribution of litter due to the steep slope at  
354 the plot (Kobler et al. 2019). This heterogeneity is more effectively captured in the manual  
355 measurement (n=30) than by the automated chambers (n=6). In summary, we conclude that the  
356 spatial variation in CO<sub>2</sub> fluxes was higher at both sites than the difference in fluxes caused by the  
357 measurement devices (Figure 3).

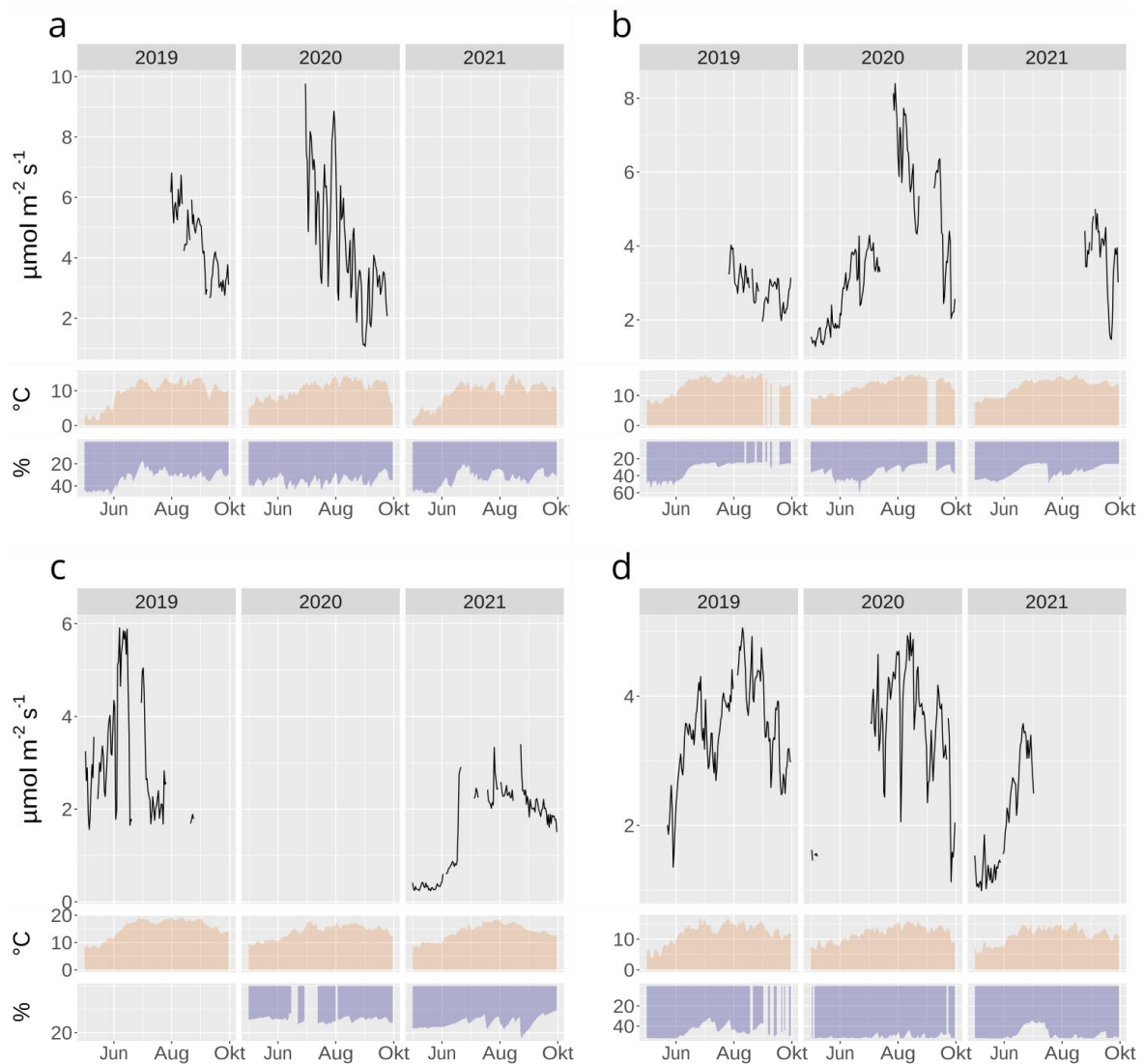
358



359

360 *Figure 3.* Comparison of automated and manual soil CO<sub>2</sub> fluxes at Klausen-Leopoldsdorf (a) and Zöbelboden (b). See *Table 3*  
361 for the specification of automated chamber data. Error bars indicate spatial variation (standard deviations).

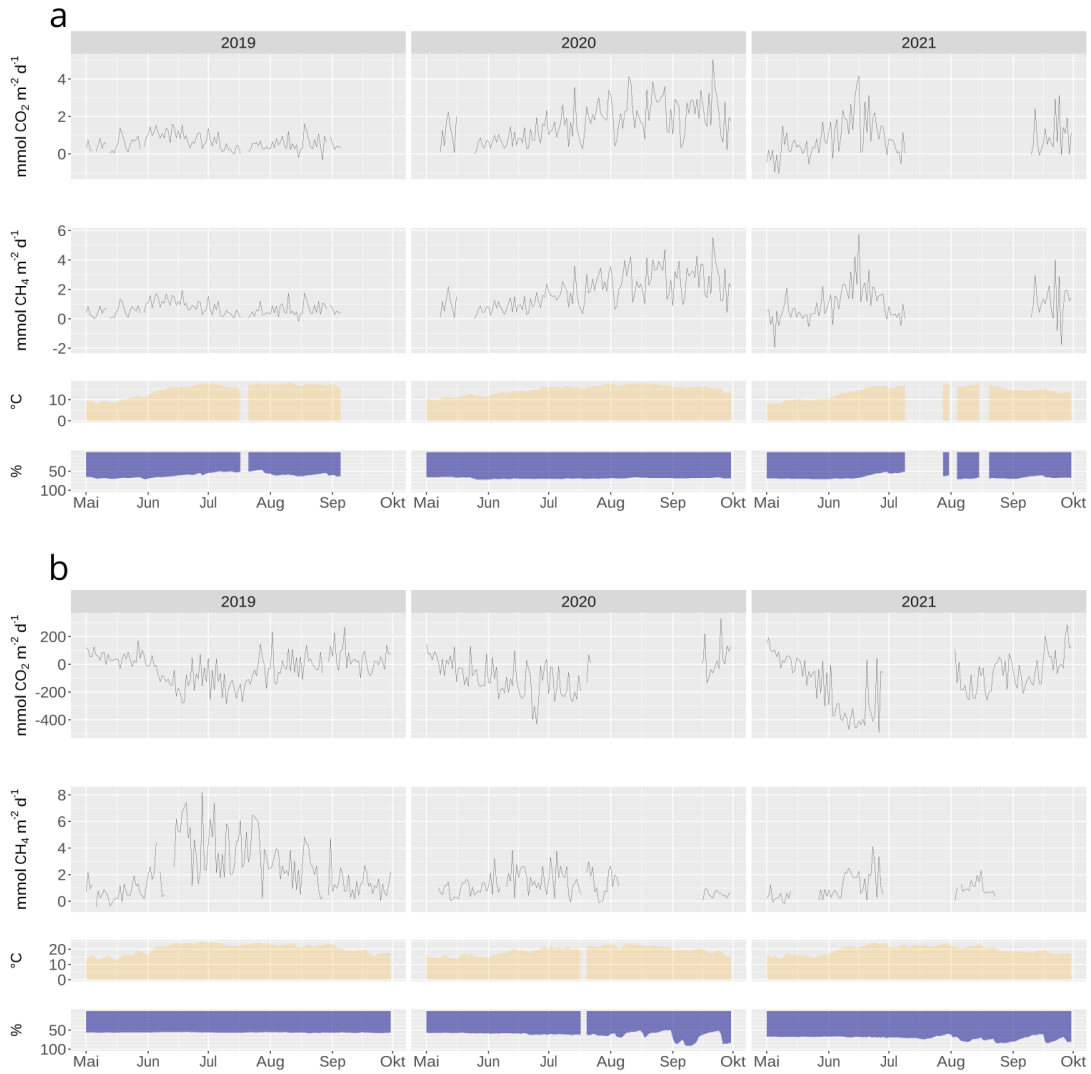
362



363

364 *Figure 4. Soil CO<sub>2</sub> respiration (mean of all chambers), soil temperature (mean of sensors in 5-15 cm depth) and soil water*  
 365 *content (mean of sensors in 5-15 cm depth) in the forested sites Stubai-Kaserstattalm (a), Klausen-Leopoldsdorf (b), Rosalia*  
 366 *(c), and Zöbelboden (d).*

367 Soil CO<sub>2</sub> fluxes are temperature dependent, thus follow the seasonal changes in soil temperature  
 368 (Figure 4). Their additional limitation through soil water availability for plant metabolism and  
 369 microbial activity is usually much less pronounced in these temperate zone ecosystems (Bahn et al.  
 370 2008; Chen et al. 2014). For detailed interpretation of the CO<sub>2</sub> respiration fluxes and their limiting  
 371 factors, we refer to the citations listed in the site description chapter. Drollinger et al. (2019)  
 372 provides interpretations of the patterns of CO<sub>2</sub> and CH<sub>4</sub> fluxes, measured using Eddy covariance  
 373 techniques at the bog site Pürgschachen Moor (PUE), and likewise, Baur et al. (2024), for the reed  
 374 belt of Neusiedler See (NSS). Stem growth limitations can, on the other hand, be closely related to  
 375 soil water content, particularly at sites with relatively low precipitation such as Klausen-Leopoldsdorf  
 376 (KLL) (Figure 6). For an in-depth study of drought related effects on tree growth at the treeline forest  
 377 at Kasterstattalm (KAS), we refer to Oberleitner et al. (2022).



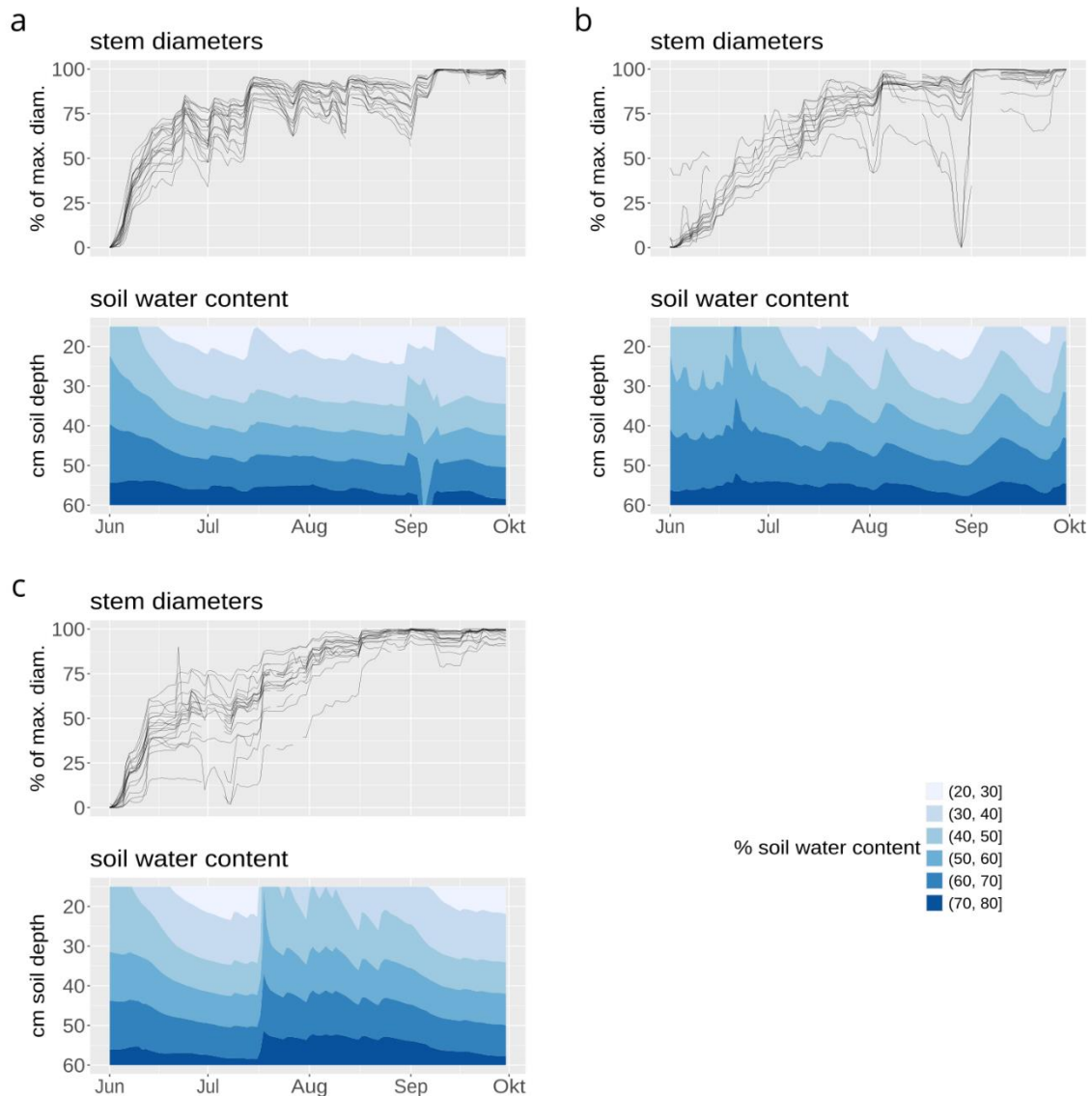
378

379

380

*Figure 5. CO<sub>2</sub> and CH<sub>4</sub> fluxes in the sites Pürgschachen Moor peat bog (a) and Lake Neusiedl reed zone (b) as well as soil temperature and soil water content.*

381



382

383 *Figure 6.* Relative stem diameters and soil moisture at the site Klausen-Leopoldsdorf during the years 2019 (a), 2020 (b),  
 384 and 2021 (c). Stem diameter values were scaled to an annual amplitude of 100.

385

## 386 6. Discussion

387 We provide baseline ecosystem data related to the carbon cycle and capture naturally occurring ECEs  
 388 across various ecosystem types typical for Austria and other regions of Central Europe. Such data sets  
 389 are scarce because the measurements are demanding in terms of maintenance and funding.

390 Automated soil respiration data in high temporal resolution, as we report it here, is rare too owing to  
 391 a lack of dedicated monitoring or research infrastructures (Bond-Lamberty et al., 2021). However,  
 392 soil CO<sub>2</sub> respiration constitutes the second-largest flux in the global carbon cycle, hence is key in  
 393 estimating ecosystem response to ECEs (Bond-Lamberty and Thomson, 2010). In addition, we  
 394 provide soil temperature and moisture measurements in the same resolution, being key variables  
 395 determining soil respiration (Pumpanen et al., 2015). High-resolution measurements of tree stem  
 396 circumference have been developed as complementary data to relate drought stress with changes in  
 397 carbon allocation in trees (Zweifel, 2016; Zweifel et al., 2021). The microclimatic, soil, and tree

398 physiological data is complemented by CO<sub>2</sub> and CH<sub>4</sub> fluxes between the vegetation and the  
399 atmosphere measured with Eddy covariance techniques of the two wetland sites.

400 Our data is particularly useful for drought-related research. Triggered by the pan-European drought  
401 of 2003 (Ciais et al., 2005), a key scientific question has been how droughts affect greenhouse gas  
402 sinks and sources in ecosystems (Rödenbeck et al., 2020; Reichstein et al., 2013; Anderegg et al.,  
403 2020). Droughts usually reduce soil respiration due to the decrease in autotrophic respiration but  
404 also because soil microbial activity drops due to water limitation (Grünzweig et al., 2022).  
405 Furthermore, rewetting can result in pulses of high soil respiration (Borken and Matzner, 2009).  
406 Drought effects on the ecosystem C cycle can persist for years (Kannenbergh et al., 2020; Müller and  
407 Bahn, 2022) and novel approaches are being developed for assimilating high-resolution data for  
408 understanding and quantifying such legacies (Yu et al., 2022; Fu et al., 2020). In this context, the  
409 availability of long-term, high-resolution measurements of key ecosystem parameters is key for  
410 understanding and quantifying the effects of recurrent droughts (Oberleitner et al., 2022). While the  
411 three-year data with the usual measurement gaps occurring in field campaigns in rather difficult  
412 terrain can only to some extent capture aspects of drought related effects, it represents a valuable  
413 baseline.

414

415 The sites presented here are currently being upgraded towards their implementation in the  
416 European Research Infrastructure for Integrated European Long-Term Ecosystem, critical zone and  
417 socio-ecological Research (eLTER RI), together with another ~200 sites in Europe (Mirtl et al., 2018).  
418 Climate change impacts on ecosystem processes including the carbon cycle are among the targeted  
419 research areas the eLTER RI will focus on. The measurements resulting in the data presented here  
420 will continue in future under the umbrella of eLTER RI. Compiling longer-term data series depends  
421 upon the availability of already validated data sets - as it is presented here - before the RI is being  
422 operational. Furthermore, long-term ecosystem observations already exist in these sites with regard  
423 to water and nitrogen cycle allowing for a contextual interpretation of the trends seen in C related  
424 parameters.

425 Combining several research and monitoring activities at already heavily instrumented sites not only  
426 saves money but widens the data analyses portfolio (Futter et al. 2023; Kulmala 2018). Even though  
427 we provide Eddy covariance data for two of our sites, Austria is not part of the Integrated Carbon  
428 Observation System (ICOS). A combination of data capturing long-term boundary layer exchange of C  
429 together with soil C fluxes, microclimate, and, in forests, tree physiological data obviously holds great  
430 potential (Zweifel et al., 2023; Ramonet et al., 2020). Hence, using the sites simultaneously for other  
431 research infrastructures, such as ICOS, providing high-quality Eddy covariance measurements would  
432 obviously be ideal. The more so because European Research Infrastructures follow the FAIR data  
433 principles to make data Findable, Accessible, Interoperable and Reusable (Wilkinson et al., 2016).

434 While the eLTER RI data infrastructure is still under development, we comply with the standards  
435 already implemented. We used DEIMS-SDR (<https://deims.org/>) as the catalogue documenting the  
436 sites (Wohner et al., 2019; Wohnner et al., 2022). It issues persistent identifiers for sites (see Table 1)  
437 that allow to uniquely identify sites across research projects and networks. Tools are being  
438 developed to query available information about sites programmatically (Oggioni et al., 2023;  
439 Wohnner, 2023) providing contextual ecosystem information.

440

441 7. Data availability



442 7.1 Data access

443 The data and metadata is accessible at B2SHARE (<https://b2share.eudat.eu/>), a service provided by  
 444 the EUDAT Collaborative Data Infrastructure. DOIs of the datasets are listed in Table 5. The site  
 445 metadata in DEIMS-SDR (Table 1) is part of the data metadata so that site information can easily be  
 446 accessed. In chapter8, we provide a jupyter notebook to download and merge the single datasets,  
 447 and to visualize parameters.

448 *Table 5. Dataset DOIs*

| Site                                      | Dataset                             | DOI   | Reference                     |
|---|-------------------------------------|---|-------------------------------|
| Klausen-<br>Leopoldsdorf                  | Meteorology                         | <a href="https://doi.org/10.23728/b2share.8f872a37513c4768b16ce755eca4bb57">https://doi.org/10.23728/b2share.8f872a37513c4768b16ce755eca4bb57</a> | (Gartner et al., 2024a)       |
|   | Soil climate                        | <a href="https://doi.org/10.23728/b2share.8d49c0b557f1455a9e66689e035b8cce">https://doi.org/10.23728/b2share.8d49c0b557f1455a9e66689e035b8cce</a> | (Gartner et al., 2024b)       |
|   | Soil CO <sub>2</sub><br>respiration | <a href="https://doi.org/10.23728/b2share.5286bd1bc6aa491f874b9bb12d1c5673">https://doi.org/10.23728/b2share.5286bd1bc6aa491f874b9bb12d1c5673</a> | (Kitzler and Hofbauer, 2024)  |
|   | Stem<br>increment                   | <a href="https://doi.org/10.23728/b2share.68d84a913f0c4875be5c680ad4d6959e">https://doi.org/10.23728/b2share.68d84a913f0c4875be5c680ad4d6959e</a> | (Gartner and Gollobich, 2024) |
| Rosalia Forest<br>Demonstration<br>Centre | Meteorology                         | <a href="https://doi.org/10.23728/b2share.96c52c247eb846deb2a3ec5e2c27b4f1">https://doi.org/10.23728/b2share.96c52c247eb846deb2a3ec5e2c27b4f1</a> | (Diaz-Pines, 2024a)           |
|   | Soil climate                        | <a href="https://doi.org/10.23728/b2share.c68143fc11224c44ae5529bd6a35a76d">https://doi.org/10.23728/b2share.c68143fc11224c44ae5529bd6a35a76d</a> | (Diaz-Pines, 2024c)           |
|   | Soil CO <sub>2</sub><br>respiration | <a href="https://doi.org/10.23728/b2share.d167e727abe947abbc8efc04057557f6">https://doi.org/10.23728/b2share.d167e727abe947abbc8efc04057557f6</a> | (Diaz-Pines, 2024b)           |
|   | Stem<br>increment                   | <a href="https://doi.org/10.23728/b2share.d0d185f1eb184ae48f6d06ea9aa8dbdf">https://doi.org/10.23728/b2share.d0d185f1eb184ae48f6d06ea9aa8dbdf</a> | (Diaz-Pines, 2024d)           |
| Zöbelboden                                | Meteorology                         | <a href="https://doi.org/10.23728/b2share.762e665273234b129d09ef017416bcfb">https://doi.org/10.23728/b2share.762e665273234b129d09ef017416bcfb</a> | (Kobler et al., 2024a)        |
|   | Soil climate                        | <a href="https://doi.org/10.23728/b2share.46e19191ce9c427d90f48ce38f56a0e1">https://doi.org/10.23728/b2share.46e19191ce9c427d90f48ce38f56a0e1</a> | (Kobler et al., 2024c)        |
|   | Soil CO <sub>2</sub><br>respiration | <a href="https://doi.org/10.23728/b2share.4f44006b932142e68981106a016f1f56">https://doi.org/10.23728/b2share.4f44006b932142e68981106a016f1f56</a> | (Kobler et al., 2024b)        |
|   | Stem<br>increment                   | <a href="https://doi.org/10.23728/b2share.2de5b37a0cad4f82a19f477531d6af24">https://doi.org/10.23728/b2share.2de5b37a0cad4f82a19f477531d6af24</a> | (Pröll et al., 2024)          |
| Stubai -<br>Kaserstattalm                 | Meteorology                         | <a href="https://doi.org/10.23728/b2share.77462914dc0b43cb8c24a967e6851665">https://doi.org/10.23728/b2share.77462914dc0b43cb8c24a967e6851665</a> | (Ingrisch and Bahn, 2024c)    |
|   | Soil climate                        | <a href="https://doi.org/10.23728/b2share.026d76094e8f4512b09b35b7a0d2a9d7">https://doi.org/10.23728/b2share.026d76094e8f4512b09b35b7a0d2a9d7</a> | (Ingrisch and Bahn, 2024d)    |
|   | Soil CO <sub>2</sub><br>respiration | <a href="https://doi.org/10.23728/b2share.cfe8c7ad1965433484650ea9026512ca">https://doi.org/10.23728/b2share.cfe8c7ad1965433484650ea9026512ca</a> | (Ingrisch and Bahn, 2024a)    |
|   | Stem<br>increment                   | <a href="https://doi.org/10.23728/b2share.0e3eed54ff30418f8720806b5f05cca9">https://doi.org/10.23728/b2share.0e3eed54ff30418f8720806b5f05cca9</a> | (Ingrisch and Bahn, 2024b)    |
| Pürgschachen<br>Moor                      | Meteorology                         | <a href="https://doi.org/10.23728/b2share.5442510ad03e4968afb4e2108e85a64d">https://doi.org/10.23728/b2share.5442510ad03e4968afb4e2108e85a64d</a> | (Maier and Glatzel, 2024e)    |
|   | Soil climate                        | <a href="https://doi.org/10.23728/b2share.9380364098d14978b876a87517652d62">https://doi.org/10.23728/b2share.9380364098d14978b876a87517652d62</a> | (Maier and Glatzel, 2024f)    |
|   | Eddy<br>Covariance                  | <a href="https://doi.org/10.23728/b2share.4f783e3ff2884abca5c59960db0b7955">https://doi.org/10.23728/b2share.4f783e3ff2884abca5c59960db0b7955</a> | (Maier and Glatzel, 2024d)    |
| Lake Neusiedl                             | Meteorology                         | <a href="https://doi.org/10.23728/b2share.f7176c9ee982464f947d2fe9fb8f389d">https://doi.org/10.23728/b2share.f7176c9ee982464f947d2fe9fb8f389d</a> | (Maier and Glatzel, 2024b)    |
|   | Soil climate                        | <a href="https://doi.org/10.23728/b2share.4e6474cd55f9487d97e3d31e83baa530">https://doi.org/10.23728/b2share.4e6474cd55f9487d97e3d31e83baa530</a> | (Maier and Glatzel, 2024c)    |

449

## 450 7.2 Data visualization, workflow integration

451 The software stack used to store, import and quality control the provided data is built on PostgreSQL  
452 database with a Post-GIS extension. The database structure is derived from the Time Series  
453 Management (TSM) system developed by the Research Center Jülich (Wohner, C., Dirnböck, T.,  
454 Peterseil, J., Pröll, G., Geiger, S., 2021) and originally deployed during the LTER CWN project but was  
455 repurposed to better fit the needs of the data management and working group. Now, for the import  
456 and quality control of data, a number of Python scripts deployed in a Jupyter environment are used.  
457 This is also includes scripts to visualise the data on the fly in Jupyter.

458

## 459 8. Code availability

460 A Jupyter notebook to access, merge, and visualize the data from all sites is available at  
461 <https://gist.github.com/10/9bbe44a03f12801c6c742202b005db57>.

462

## 463 9. Author contribution

464 DT, BM, DPM, DI, EM, GK, GG, MA, IJ, KB, KJ, MA, PG, VS, ZBS, ZA, and GS designed the  
465 measurements and carried them out. WC, PJ designed and constructed the database. KK, VS, and PG  
466 customized and filled the database. OI developed the Jupyter notebook. DT prepared the manuscript  
467 with contributions from all co-authors.

468

## 469 10. Competing interests

470 The authors declare that they have no conflict of interest.

471

## 472 11. Acknowledgements

473 We want to thank Manfred Bogner, Thomas Lehner, Christian Holtermann, Thomas Kager, and Josef  
474 Gasch for technical implementation and assistance.

475

## 476 12. Funding

477 The infrastructure and its implementation was funded by the Austrian Research Promotion Agency  
478 (FFG, project LTER-CWN: Long-Term Ecosystem Research Infrastructure for Carbon, Water and  
479 Nitrogen, grant no. 858024). The Austrian Academy of Sciences (ÖAW) supported all authors for data  
480 compilation and writing of the manuscript through its eLTER 2022 call (Earth System Sciences (ESS)).  
481 T.D., J.K., K.K., J.P., C.W. and E.D-P. received additional funding from the EU Horizon 2020 project  
482 eLTER PLUS (grant no. 871128), and E.D-P. also from the project EXAFOR (Austrian Climate Research  
483 Programme 12th Call, grant no. KR19AC0K17557).

484

485 13. References

- 486 Anderegg, W. R. L., Trugman, A. T., Badgley, G., Anderson, C. M., Bartuska, A., Ciais, P., Cullenward,  
 487 D., Field, C. B., Freeman, J., Goetz, S. J., Hicke, J. A., Huntzinger, D., Jackson, R. B., Nickerson, J.,  
 488 Pacala, S., and Randerson, J. T.: Climate-driven risks to the climate mitigation potential of forests,  
 489 Science, 368, eaaz7005, <https://doi.org/10.1126/science.aaz7005>, 2020.
- 490 Baatz, R., Hendricks Franssen, H. J., Euskirchen, E., Sihi, D., Dietze, M., Ciavatta, S., Fennel, K., Beck,  
 491 H., Lannoy, G. de, Pauwels, V. R. N., Raiho, A., Montzka, C., Williams, M., Mishra, U., Poppe, C.,  
 492 Zacharias, S., Lausch, A., Samaniego, L., van Looy, K., Bogena, H., Adamescu, M., Mirtl, M., Fox, A.,  
 493 Goergen, K., Naz, B. S., Zeng, Y., and Vereecken, H.: Reanalysis in Earth System Science: Toward  
 494 Terrestrial Ecosystem Reanalysis, Reviews of Geophysics, 59,  
 495 <https://doi.org/10.1029/2020RG000715>, 2021.
- 496 Bahn, M. and Ingrisch, J.: Accounting for Complexity in Resilience Comparisons: A Reply to Yeung and  
 497 Richardson, and Further Considerations, Trends in Ecology & Evolution, 33, 649–651,  
 498 <https://doi.org/10.1016/j.tree.2018.06.006>, 2018.
- 499 Bahn, M., Rodeghiero, M., Anderson-Dunn, M., Dore, S., Gimeno, C., Drösler, M., Williams, M.,  
 500 Ammann, C., Berninger, F., Flechard, C., Jones, S., Balzarolo, M., Kumar, S., Newesely, C.,  
 501 Priwitzer, T., Raschi, A., Siegwolf, R., Susiluoto, S., Tenhunen, J., Wohlfahrt, G., and Cernusca, A.:  
 502 Soil Respiration in European Grasslands in Relation to Climate and Assimilate Supply, Ecosystems,  
 503 11, 1352–1367, <https://doi.org/10.1007/s10021-008-9198-0>, 2008.
- 504 Bahn, M., Schmitt, M., Siegwolf, R., Richter, A., and Brüggemann, N.: Does photosynthesis affect  
 505 grassland soil-respired CO<sub>2</sub> and its carbon isotope composition on a diurnal timescale?, New  
 506 Phytologist, 182, 451–460, <https://doi.org/10.1111/j.1469-8137.2008.02755.x>, 2009.
- 507 Baur, P. A., Henry Pinilla, D., and Glatzel, S.: Is ebullition or diffusion more important as methane  
 508 emission pathway in a shallow subsaline lake?, Science of The Total Environment, 912, 169112,  
 509 <https://doi.org/10.1016/j.scitotenv.2023.169112>, 2024.
- 510 Bernal, S., Hedin, L. O., Likens, G. E., Gerber, S., and Buso, D. C.: Complex response of the forest  
 511 nitrogen cycle to climate change, Proceedings of the National Academy of Sciences, 109, 3406–  
 512 3411, <https://doi.org/10.1073/pnas.1121448109>, 2012.
- 513 Bond-Lamberty, B. and Thomson, A.: Temperature-associated increases in the global soil respiration  
 514 record, Nature, 464, 579–582, 2010.
- 515 Bond-Lamberty, B., Christianson, D. S., Crystal-Ornelas, R., Mathes, K., and Pennington, S. C.: A  
 516 reporting format for field measurements of soil respiration, Ecological Informatics, 62, 101280,  
 517 <https://doi.org/10.1016/j.ecoinf.2021.101280>, 2021.
- 518 Borken, W. and Matzner, E.: Reappraisal of drying and wetting effects on C and N mineralization and  
 519 fluxes in soil, Global Change Biology, 15, 808–824, 2009.
- 520 Buchsteiner, C., Baur, P. A., and Glatzel, S.: Spatial Analysis of Intra-Annual Reed Ecosystem Dynamics  
 521 at Lake Neusiedl Using RGB Drone Imagery and Deep Learning, Remote Sensing, 15, 3961,  
 522 <https://doi.org/10.3390/rs15163961>, 2023.
- 523 Chen, S., Zou, J., Hu, Z., Chen, H., and Lu, Y.: Global annual soil respiration in relation to climate, soil  
 524 properties and vegetation characteristics: Summary of available data, Agricultural and Forest  
 525 Meteorology, 198-199, 335–346, <https://doi.org/10.1016/j.agrformet.2014.08.020>, 2014.
- 526 Ciais, P., Reichstein, M., Viovy, N., Granier, A., Ogée, J., Allard, V., Aubinet, M., Buchmann, N.,  
 527 Bernhofer, C., Carrara, A., Chevallier, F., Noblet, N. de, Friend, A. D., Friedlingstein, P., Grünwald,  
 528 T., Heinesch, B., Keronen, P., A. Knohl, A., Krinner, G., Loustau, D., Manca, G., Matteucci, G.,  
 529 Miglietta, F., Ourcival, J. M., Papale, D., Pilegaard, K., Rambal, S., Seufert, G., Soussana, J. F., M. J.  
 530 Sanz, Schulze, E.-D., Vesala, T., and Valentini, R.: Europe-wide reduction in primary productivity  
 531 caused by the heat and drought in 2003, Nature, 437, 529–533, 2005.

532 Diaz-Pines, E.: Rosalia forest (Austria) - meteorological data (2020-2021),  
533 <https://doi.org/10.23728/B2SHARE.96C52C247EB846DEB2A3EC5E2C27B4F1>, 2024a.

534 Diaz-Pines, E.: Rosalia forest (Austria) - soil CO2 respiration (2019-2021),  
535 <https://doi.org/10.23728/B2SHARE.D167E727ABE947ABBC8EFC04057557F6>, 2024b.

536 Diaz-Pines, E.: Rosalia forest (Austria) - soil temperature and soil moisture (2019-2021),  
537 <https://doi.org/10.23728/B2SHARE.C68143FC11224C44AE5529BD6A35A76D>, 2024c.

538 Diaz-Pines, E.: Rosalia forest (Austria) - tree increments (2019-2021),  
539 <https://doi.org/10.23728/B2SHARE.D0D185F1EB184AE48F6D06EA9AA8DBDF>, 2024d.

540 Dirnböck, T., Brielmann, H., Djukic, I., Geiger, S., Hartmann, A., Humer, F., Kobler, J., Kralik, M., Liu, Y.,  
541 Mirtl, M., and Pröll, G.: Long- and Short-Term Inorganic Nitrogen Runoff from a Karst Catchment  
542 in Austria, *Forests*, 11, 1112, <https://doi.org/10.3390/f11101112>, 2020.

543 Dirnböck, T., Haase, P., Mirtl, M., Pauw, J., and Templer, P. H.: Contemporary International Long-  
544 Term Ecological Research (ILTER)—from biogeosciences to socio-ecology and biodiversity  
545 research, *Reg Environ Change*, 19, 309–311, <https://doi.org/10.1007/s10113-018-1445-0>, 2019.

546 Dirnböck, T., Kobler, J., Kraus, D., Grote, R., and Kiese, R.: Impacts of management and climate  
547 change on nitrate leaching in a forested karst area, *Journal of Environmental Management*, 165,  
548 243–252, <https://doi.org/10.1016/j.jenvman.2015.09.039>, 2016.

549 Drollinger, S., Maier, A., and Glatzel, S.: Interannual and seasonal variability in carbon dioxide and  
550 methane fluxes of a pine peat bog in the Eastern Alps, Austria, *Agricultural and Forest  
551 Meteorology*, 275, 69–78, <https://doi.org/10.1016/j.agrformet.2019.05.015>, 2019.

552 Frank, D., Reichstein, M., Bahn, M., Thonicke, K., Frank, D., Mahecha, M. D., Smith, P., van der Velde,  
553 M., Vicca, S., Babst, F., Beer, C., Buchmann, N., Canadell, J. G., Ciais, P., Cramer, W., Ibrom, A.,  
554 Miglietta, F., Poulter, B., Rammig, A., Seneviratne, S. I., Walz, A., Wattenbach, M., Zavala, M. A.,  
555 and Zscheischler, J.: Effects of climate extremes on the terrestrial carbon cycle: concepts,  
556 processes and potential future impacts, *Global Change Biology*, 21, 2861–2880,  
557 <https://doi.org/10.1111/gcb.12916>, 2015.

558 Fu, Z., Ciais, P., Bastos, A., Stoy, P. C., Yang, H., Green, J. K., Wang, B., Yu, K., Huang, Y., Knohl, A.,  
559 Šigut, L., Gharun, M., Cuntz, M., Arriga, N., Roland, M., Peichl, M., Migliavacca, M., Cremonese, E.,  
560 Varlagin, A., Brümmer, C., La Gourlez de Motte, L., Fares, S., Buchmann, N., El-Madany, T. S.,  
561 Pitacco, A., Vendrame, N., Li, Z., Vincke, C., Magliulo, E., and Koepsch, F.: Sensitivity of gross  
562 primary productivity to climatic drivers during the summer drought of 2018 in Europe,  
563 *Philosophical transactions of the Royal Society of London. Series B, Biological sciences*, 375,  
564 20190747, <https://doi.org/10.1098/rstb.2019.0747>, 2020.

565 Fuchslueger, L., Bahn, M., Fritz, K., Hasibeder, R., and Richter, A.: Experimental drought reduces the  
566 transfer of recently fixed plant carbon to soil microbes and alters the bacterial community  
567 composition in a mountain meadow, *New Phytologist*, 201, 916–927,  
568 <https://doi.org/10.1111/nph.12569>, 2014.

569 Fürst, J., Nachtnebel, H. P., Gasch, J., Nolz, R., Stockinger, M. P., Stumpp, C., and Schulz, K.: Rosalia:  
570 an experimental research site to study hydrological processes in a forest catchment, *Earth Syst.  
571 Sci. Data*, 13, 4019–4034, <https://doi.org/10.5194/essd-13-4019-2021>, 2021.

572 Fuss, R.: gasfluxes: greenhouse gas flux calculation from chamber measurements, 2020.

573 Futter, M. N., Dirnböck, T., Forsius, M., Bäck, J. K., Cools, N., Diaz-Pines, E., Dick, J., Gaube, V.,  
574 Gillespie, L. M., Högbom, L., Laudon, H., Mirtl, M., Nikolaidis, N., Poppe Terán, C., Skiba, U.,  
575 Vereecken, H., Villwock, H., Weldon, J., Wohner, C., and Alam, S. A.: Leveraging research  
576 infrastructure co-location to evaluate constraints on terrestrial carbon cycling in northern  
577 European forests, *Ambio*, 52, 1819–1831, <https://doi.org/10.1007/s13280-023-01930-4>, 2023.

578 Gartner, K. and Gollobich, G.: Klausen-Leopoldsdorf (Austria) - tree increments (2019-2021),  
579 <https://doi.org/10.23728/B2SHARE.68D84A913F0C4875BE5C680AD4D6959E>, 2024.

580 Gartner, K., Gollobich, G., and Zolles, A.: Klausen-Leopoldsdorf (Austria) - meteorological data (2019-  
581 2021), <https://doi.org/10.23728/B2SHARE.8F872A37513C4768B16CE755ECA4BB57>, 2024a.

582 Gartner, K., Gollobich, G., and Zolles, A.: Klausen-Leopoldsdorf (Austria) - soil temperature and soil  
583 moisture (2019-2021),  
584 <https://doi.org/10.23728/B2SHARE.8D49C0B557F1455A9E66689E035B8CCE>, 2024b.

585 Gillespie, L. M., Kolari, P., Kulmala, L., Leitner, S. M., Pihlatie, M., Zechmeister-Boltenstern, S., and  
586 Díaz-Pinés, E.: Drought effects on soil greenhouse gas fluxes in a boreal and a temperate forest,  
587 *Biogeochemistry*, 167, 155–175, <https://doi.org/10.1007/s10533-024-01126-2>, 2024.

588 Gillespie, L. M., Triches, N. Y., Abalos, D., Finke, P., Zechmeister-Boltenstern, S., Glatzel, S., and Díaz-  
589 Pinés, E.: Land inclination controls CO<sub>2</sub> and N<sub>2</sub>O fluxes, but not CH<sub>4</sub> uptake, in a temperate  
590 upland forest soil, *SOIL*, 9, 517–531, <https://doi.org/10.5194/soil-9-517-2023>, 2023.

591 Glatzel, S., Worrall, F., Boothroyd, I. M., and Heckman, K.: Comparison of the transformation of  
592 organic matter flux through a raised bog and a blanket bog, *Biogeochemistry*,  
593 <https://doi.org/10.1007/s10533-023-01093-0>, 2023.

594 Gollob, C., Ritter, T., and Nothdurft, A.: Comparison of 3D Point Clouds Obtained by Terrestrial Laser  
595 Scanning and Personal Laser Scanning on Forest Inventory Sample Plots, *Data*, 5, 103,  
596 <https://doi.org/10.3390/data5040103>, 2020.

597 Grünzweig, J. M., Boeck, H. J. de, Rey, A., Santos, M. J., Adam, O., Bahn, M., Belnap, J., Deckmyn, G.,  
598 Dekker, S. C., Flores, O., Gliksmann, D., Helman, D., Hultine, K. R., Liu, L., Meron, E., Michael, Y.,  
599 Sheffer, E., Throop, H. L., Tzuk, O., and Yakir, D.: Dryland mechanisms could widely control  
600 ecosystem functioning in a drier and warmer world, *Nat Ecol Evol*, 6, 1064–1076,  
601 <https://doi.org/10.1038/s41559-022-01779-y>, 2022.

602 Hartl-Meier, C., Zang, C., Büntgen, U., Esper, J., Rothe, A., Göttlein, A., Dirnböck, T., and Treydte, K.:  
603 Uniform climate sensitivity in tree-ring stable isotopes across species and sites in a mid-latitude  
604 temperate forest, *Tree Physiology*, <https://doi.org/10.1093/treephys/tpu096>, 2014.

605 Hasibeder, R., Fuchslueger, L., Richter, A., and Bahn, M.: Summer drought alters carbon allocation to  
606 roots and root respiration in mountain grassland, *New Phytologist*, 205, 1117–1127,  
607 <https://doi.org/10.1111/nph.13146>, 2015.

608 Haslinger, K., Bartsch, A.: Creating long-term gridded fields of reference evapotranspiration in Alpine  
609 terrain based on a recalibrated Hargreaves method. *Hydrology and Earth System Sciences*, 20,  
610 1211–1223, <https://hess.copernicus.org/articles/20/1211/2016/>, 2016.

611 Heimann, M. and Reichstein, M.: Terrestrial ecosystem carbon dynamics and climate feedbacks,  
612 *Nature*, 451, 289–292, 2008.

613 Hutchinson, G. L. and Mosier, A. R.: Improved Soil Cover Method for Field Measurement of Nitrous  
614 Oxide Fluxes, *Soil Sci. Soc. Am. j.*, 45, 311–316,  
615 <https://doi.org/10.2136/sssaj1981.03615995004500020017x>, 1981.

616 Ingrisich, J. and Bahn, M.: Kaserstattalm (Austria) - forest soil CO<sub>2</sub> respiration (2019-2020),  
617 <https://doi.org/10.23728/B2SHARE.CFE8C7AD1965433484650EA9026512CA>, 2024a.

618 Ingrisich, J. and Bahn, M.: Kaserstattalm (Austria) - forest tree increments (2019-2021),  
619 <https://doi.org/10.23728/B2SHARE.OE3EED54FF30418F8720806B5F05CCA9>, 2024b.

620 Ingrisich, J. and Bahn, M.: Kaserstattalm (Austria) - meteorological data (2019-2021),  
621 <https://doi.org/10.23728/B2SHARE.77462914DC0B43CB8C24A967E6851665>, 2024c.

622 Ingrisich, J. and Bahn, M.: Kaserstattalm (Austria) - soil temperature and soil moisture (2019-2021),  
623 <https://doi.org/10.23728/B2SHARE.026D76094E8F4512B09B35B7A0D2A9D7>, 2024d.

624 Ingrisich, J. and Bahn, M.: Towards a Comparable Quantification of Resilience, *Trends in Ecology &*  
625 *Evolution*, 33, 251–259, <https://doi.org/10.1016/j.tree.2018.01.013>, 2018.

626 Ingrisich, J., Karlowsky, S., Hasibeder, R., Gleixner, G., and Bahn, M.: Drought and recovery effects on  
627 belowground respiration dynamics and the partitioning of recent carbon in managed and  
628 abandoned grassland, *Glob Chang Biol*, 26, 4366–4378, <https://doi.org/10.1111/gcb.15131>, 2020.

629 Ingrisich, J., Karlowsky, S., Anadon-Rosell, A., Hasibeder, R., König, A., Augusti, A., Gleixner, G., and  
630 Bahn, M.: Land Use Alters the Drought Responses of Productivity and CO<sub>2</sub> Fluxes in Mountain  
631 Grassland, *Ecosystems*, 21, 689–703, <https://doi.org/10.1007/s10021-017-0178-0>, 2018.

632 IPCC: Climate Change 2021: The Physical Science Basis: Contribution of Working Group I to the Sixth  
633 Assessment Report of the Intergovernmental Panel on Climate Change, Cambridge University  
634 Press, Cambridge, United Kingdom and New York, NY, USA, 2021.

635 Kannenberg, S. A., Schwalm, C. R., and Anderegg, W. R. L.: Ghosts of the past: how drought legacy  
636 effects shape forest functioning and carbon cycling, *Ecology Letters*, 23, 891–901,  
637 <https://doi.org/10.1111/ele.13485>, 2020.

638 Kitzler, B., Zechmeister-Boltenstern, S., Holtermann, C., Skiba, U., and Butterbach-Bahl, K.: Controls  
639 over N<sub>2</sub>O, NO<sub>x</sub> and CO<sub>2</sub> fluxes in a calcareous mountain forest soil, *Biogeosciences*, 3, 383–395,  
640 2006.

641 Kitzler, B. and Hofbauer, A.: Klausen-Leopoldsdorf (Austria) - soil CO<sub>2</sub> respiration for the years (2019-  
642 2020), <https://doi.org/10.23728/B2SHARE.5286BD1BC6AA491F874B9BB12D1C5673>, 2024.

643 Knierzinger, W., Drescher-Schneider, R., Knorr, K.-H., Drollinger, S., Limbeck, A., Brunnbauer, L.,  
644 Horak, F., Festi, D., and Wagleich, M.: Anthropogenic and climate signals in late-Holocene peat  
645 layers of an ombrotrophic bog in the Styrian Enns valley (Austrian Alps), *E&G Quaternary Sci. J.*,  
646 69, 121–137, <https://doi.org/10.5194/egqsj-69-121-2020>, 2020.

647 Kobler, J., Dirnböck, T., and Pröll, G.: Zöbelboden (Austria) - meteorological data (2019-2021),  
648 <https://doi.org/10.23728/B2SHARE.762E665273234B129D09EF017416BCFB>, 2024a.

649 Kobler, J., Dirnböck, T., and Pröll, G.: Zöbelboden (Austria) - soil CO<sub>2</sub> respiration for the years (2019-  
650 2021), <https://doi.org/10.23728/B2SHARE.4F44006B932142E68981106A016F1F56>, 2024b.

651 Kobler, J., Dirnböck, T., and Pröll, G.: Zöbelboden (Austria) - soil temperature and soil moisture (2019-  
652 2021), <https://doi.org/10.23728/B2SHARE.46E19191CE9C427D90F48CE38F56A0E1>, 2024c.

653 Kobler, J., Zehetgruber, B., Dirnböck, T., Jandl, R., Mirtl, M., and Schindlbacher, A.: Effects of aspect  
654 and altitude on carbon cycling processes in a temperate mountain forest catchment, *Landscape*  
655 *Ecol*, <https://doi.org/10.1007/s10980-019-00769-z>, 2019.

656 Kröel-Dulay, G., Mojzes, A., Szitár, K., Bahn, M., Batáry, P., Beier, C., Bilton, M., Boeck, H. J. de, Dukes,  
657 J. S., Estiarte, M., Holub, P., Jentsch, A., Schmidt, I. K., Kreyling, J., Reinsch, S., Larsen, K. S.,  
658 Sternberg, M., Tielbörger, K., Tietema, A., Vicca, S., and Peñuelas, J.: Field experiments  
659 underestimate aboveground biomass response to drought, *Nature ecology & evolution*, 6, 540–  
660 545, <https://doi.org/10.1038/s41559-022-01685-3>, 2022.

661 Kulmala, M.: Build a global Earth observatory, *Nature*, 553, 21–23, <https://doi.org/10.1038/d41586-017-08967-y>, 2018.

662 Leitner, S., Dirnböck, T., Kobler, J., and Zechmeister-Boltenstern, S.: Legacy effects of drought on  
663 nitrate leaching in a temperate mixed forest on karst, *Journal of Environmental Management*,  
664 262, <https://doi.org/10.1016/j.jenvman.2020.110338>, 2020.

665 Leitner, S., Minixhofer, P., Inselsbacher, E., Keiblinger, K. M., Zimmermann, M., and Zechmeister-  
666 Boltenstern, S.: Short-term soil mineral and organic nitrogen fluxes during moderate and severe  
667 drying–rewetting events, *Applied Soil Ecology*, 114, 28–33,  
668 <https://doi.org/10.1016/j.apsoil.2017.02.014>, available at:  
669 <https://www.sciencedirect.com/science/article/pii/S0929139316303018>, 2017.

670  
671 LI-COR Biosciences: SoilFluxPro Software: Instruction manual, 2019.

672 Liu, D., Keiblinger, K. M., Leitner, S., Wegner, U., Zimmermann, M., Fuchs, S., Lassek, C., Riedel, K.,  
673 and Zechmeister-Boltenstern, S.: Response of Microbial Communities and Their Metabolic

674 Functions to Drying–Rewetting Stress in a Temperate Forest Soil, *Microorganisms*, 7,  
675 <https://doi.org/10.3390/microorganisms7050129>, 2019.

676 Mahecha, M. D., Gans, F., Sippel, S., Donges, J. F., Kaminski, T., Metzger, S., Migliavacca, M., Papale,  
677 D., Rammig, A., and Zscheischler, J.: Detecting impacts of extreme events with ecological in situ  
678 monitoring networks, *Biogeosciences*, 14, 4255–4277, <https://doi.org/10.5194/bg-14-4255-2017>,  
679 2017.

680 Maier, A. and Glatzel, S.: Lake Neusiedl (Austria) - eddy flux data (2019–2021),  
681 <https://doi.org/10.23728/B2SHARE.B83CACA3EFE44868A1ED49129B4A576A>, 2024a.

682 Maier, A. and Glatzel, S.: Lake Neusiedl (Austria) - meteorological data (2019–2021),  
683 <https://doi.org/10.23728/B2SHARE.F7176C9EE982464F947D2FE9FB8F389D>, 2024b.

684 Maier, A. and Glatzel, S.: Lake Neusiedl (Austria) - soil temperature and soil moisture (2019–2021),  
685 <https://doi.org/10.23728/B2SHARE.4E6474CD55F9487D97E3D31E83BAA530>, 2024c.

686 Maier, A. and Glatzel, S.: Puergschachen Bog (Austria) - eddy covariance data (2019–2021),  
687 <https://doi.org/10.23728/B2SHARE.4F783E3FF2884ABCA5C59960DB0B7955>, 2024d.

688 Maier, A. and Glatzel, S.: Puergschachen Bog (Austria) - meteorological data (2019–2021),  
689 <https://doi.org/10.23728/B2SHARE.5442510AD03E4968AFB4E2108E85A64D>, 2024e.

690 Maier, A. and Glatzel, S.: Puergschachen Bog (Austria) - soil temperature and soil moisture (2019–  
691 2021), <https://doi.org/10.23728/B2SHARE.9380364098D14978B876A87517652D62>, 2024f.

692 Mirtl, M., T. Borer, E., Djukic, I., Forsius, M., Haubold, H., Hugo, W., Jourdan, J., Lindenmayer, D.,  
693 McDowell, W. H., Muraoka, H., Orenstein, D. E., Pauw, J. C., Peterseil, J., Shibata, H., Wohner, C.,  
694 Yu, X., and Haase, P.: Genesis, goals and achievements of Long-Term Ecological Research at the  
695 global scale: A critical review of ILTER and future directions, *Science of The Total Environment*,  
696 626, 1439–1462, <https://doi.org/10.1016/j.scitotenv.2017.12.001>, 2018.

697 Müller, L. M. and Bahn, M.: Drought legacies and ecosystem responses to subsequent drought, *Glob  
698 Chang Biol*, 28, 5086–5103, <https://doi.org/10.1111/gcb.16270>, 2022.

699 Müller, R., Maier, A., Inselsbacher, E., Peticzka, R., Wang, G., and Glatzel, S.: <sup>13</sup>C-Labeled Artificial  
700 Root Exudates Are Immediately Respired in a Peat Mesocosm Study, *Diversity*, 14, 735,  
701 <https://doi.org/10.3390/d14090735>, 2022.

702 Neumann, M. and Starlinger, F.: The significance of different indices for stand structure and diversity  
703 in forests, *Forest Ecology and Management*, 145, 91–106, 2001.

704 Oberleitner, F., Hartmann, H., Hasibeder, R., Huang, J., Losso, A., Mayr, S., Oberhuber, W., Wieser, G.,  
705 and Bahn, M.: Amplifying effects of recurrent drought on the dynamics of tree growth and water  
706 use in a subalpine forest, *Plant, Cell & Environment*, 45, 2617–2635,  
707 <https://doi.org/10.1111/pce.14369>, 2022.

708 Oggioni, A., Silver, M., Ranghetti, L., and Tagliolato, P.: ReLTER: An Interface for the eLTER  
709 Community, <https://github.com/ropensci/ReLTER>, 2023.

710 Pröll, G., Venier, S., and Dirnböck, T.: Zöbelboden (Austria) - tree increments (2019–2021),  
711 <https://doi.org/10.23728/B2SHARE.2DE5B37A0CAD4F82A19F477531D6AF24>, 2024.

712 Pumpanen, J., Kulmala, L., Lindén, A., Kolari, P., Nikinmaa, E., and Hari, P.: Seasonal dynamics of  
713 autotrophic respiration in boreal forest soil estimated by continuous chamber measurements,  
714 2015.

715 Pumpanen, J., Kolari, P., Ilvesniemi, H., Minkkinen, K., Vesala, T., Niinistö, S., Lohila, A., Larmola, T.,  
716 Morero, M., Pihlatie, M., Janssens, I., Yuste, J. C., Grünzweig, J. M., Reth, S., Subke, J.-A., Savage,  
717 K., Kutsch, W., Østreng, G., Ziegler, W., Anthoni, P., Lindroth, A., and Hari, P.: Comparison of  
718 different chamber techniques for measuring soil CO<sub>2</sub> efflux, *Agricultural and Forest Meteorology*,  
719 123, 159–176, <https://doi.org/10.1016/j.agrformet.2003.12.001>, 2004.

720 Ramonet, M., Ciais, P., Apadula, F., Bartyzel, J., Bastos, A., Bergamaschi, P., Blanc, P. E., Brunner, D.,  
721 Di Caracciolo Torchiarolo, L., Calzolari, F., Chen, H., Chmura, L., Colomb, A., Conil, S., Cristofanelli,

722 P., Cuevas, E., Curcoll, R., Delmotte, M., Di Sarra, A., Emmenegger, L., Forster, G., Frumau, A.,  
723 Gerbig, C., Gheusi, F., Hammer, S., Haszpra, L., Hatakka, J., Hazan, L., Heliasz, M., Henne, S.,  
724 Hensen, A., Hermansen, O., Keronen, P., Kivi, R., Komínková, K., Kubistin, D., Laurent, O., Laurila,  
725 T., Lavric, J. V., Lehner, I., Lehtinen, K. E. J., Leskinen, A., Leuenberger, M., Levin, I., Lindauer, M.,  
726 Lopez, M., Myhre, C. L., Mammarella, I., Manca, G., Manning, A., Marek, M. V., Marklund, P.,  
727 Martin, D., Meinhardt, F., Mihalopoulos, N., Mölder, M., Morgui, J. A., Necki, J., O'Doherty, S.,  
728 O'Dowd, C., Ottosson, M., Philippon, C., Piacentino, S., Pichon, J. M., Plass-Duelmer, C., Resovsky,  
729 A., Rivier, L., Rodó, X., Sha, M. K., Scheeren, H. A., Sferlazzo, D., Spain, T. G., Stanley, K. M.,  
730 Steinbacher, M., Trisolino, P., Vermeulen, A., Vítková, G., Weyrauch, D., Xueref-Remy, I., Yala, K.,  
731 and Yver Kwok, C.: The fingerprint of the summer 2018 drought in Europe on ground-based  
732 atmospheric CO<sub>2</sub> measurements, *Philosophical transactions of the Royal Society of London.*  
733 *Series B, Biological sciences*, 375, 20190513, <https://doi.org/10.1098/rstb.2019.0513>, 2020.

734 Reichstein, M., Bahn, M., Ciais, P., Frank, D., Mahecha, M. D., Seneviratne, S. I., Zscheischler, J., Beer,  
735 C., Buchmann, N., Frank, D. C., Papale, D., Rammig, A., Smith, P., Thonicke, K., van der Velde, M.,  
736 Vicca, S., Walz, A., and Wattenbach, M.: Climate extremes and the carbon cycle, *Nature*, 500,  
737 287–295, <https://doi.org/10.1038/nature12350>, 2013.

738 Rödenbeck, C., Zaehle, S., Keeling, R., and Heimann, M.: The European carbon cycle response to heat  
739 and drought as seen from atmospheric CO<sub>2</sub> data for 1999-2018, *Philosophical transactions of the*  
740 *Royal Society of London. Series B, Biological sciences*, 375, 20190506,  
741 <https://doi.org/10.1098/rstb.2019.0506>, 2020.

742 Schindlbacher, A., Wunderlich, S., Borken, W., Kitzler, B., Zechmeister-Boltenstern, S., and Jandl, R.:  
743 Soil respiration under climate change: prolonged summer drought offsets soil warming effects,  
744 *Global Change Biology*, 18, 2270–2279, <https://doi.org/10.1111/j.1365-2486.2012.02696.x>, 2012.

745 Schmitt, M., Bahn, M., Wohlfahrt, G., Tappeiner, U., and Cernusca, A.: Land use affects the net  
746 ecosystem CO<sub>2</sub> exchange and its components in mountain grasslands, *Biogeosciences*, 7, 2297–  
747 2309, <https://doi.org/10.5194/bg-7-2297-2010>, 2010.

748 Schwen, A., Zimmermann, M., Leitner, S., and Woche, S. K.: Soil Water Repellency and its Impact on  
749 Hydraulic Characteristics in a Beech Forest under Simulated Climate Change, *Vadose Zone*  
750 *Journal*, 14, 1–11, <https://doi.org/10.2136/vzj2015.06.0089>, 2015.

751 Vicente-Serrano, S. M., Beguería S, and López-Moreno, J. I.: A Multiscalar Drought Index Sensitive to  
752 Global Warming: The Standardized Precipitation Evapotranspiration Index, *Journal of Climate*, 23,  
753 1696-1718, <https://doi.org/10.1175/2009JCLI2909.1>, 2010.

754 Wilkinson, M. D., Dumontier, M., Aalbersberg, I. J. J., Appleton, G., Axton, M., Baak, A., Blomberg, N.,  
755 Boiten, J.-W., da Silva Santos, L. B., Bourne, P. E., Bouwman, J., Brookes, A. J., Clark, T., Crosas,  
756 M., Dillo, I., Dumon, O., Edmunds, S., Evelo, C. T., Finkers, R., Gonzalez-Beltran, A., Gray, A. J. G.,  
757 Groth, P., Goble, C., Grethe, J. S., Heringa, J., Hoen, P. A. C., Hooft, R., Kuhn, T., Kok, R., Kok, J.,  
758 Lusher, S. J., Martone, M. E., Mons, A., Packer, A. L., Persson, B., Rocca-Serra, P., Roos, M., van  
759 Schaik, R., Sansone, S.-A., Schultes, E., Sengstag, T., Slater, T., Strawn, G., Swertz, M. A.,  
760 Thompson, M., van der Lei, J., van Mulligen, E., Velterop, J., Waagmeester, A., Wittenburg, P.,  
761 Wolstencroft, K., Zhao, J., and Mons, B.: The FAIR Guiding Principles for scientific data  
762 management and stewardship, *Scientific data*, 3, 160018, <https://doi.org/10.1038/sdata.2016.18>,  
763 2016.

764 Wohner, C.: deimsPy, <https://pypi.org/project/deims/>, 2023.

765 Wohner, C., Peterseil, J., and Klug, H.: Designing and implementing a data model for describing  
766 environmental monitoring and research sites, *Ecological Informatics*, 70, 101708,  
767 <https://doi.org/10.1016/j.ecoinf.2022.101708>, available at:  
768 <https://www.sciencedirect.com/science/article/pii/S1574954122001583>, 2022.



769 Wohner, C., Peterseil, J., Poursanidis, D., Kliment, T., Wilson, M., Mirtl, M., and Chrysoulakis, N.:  
770 DEIMS-SDR – A web portal to document research sites and their associated data, *Ecological*  
771 *Informatics*, 51, 15–24, <https://doi.org/10.1016/j.ecoinf.2019.01.005>, 2019.

772 Wohner, C., Dirnböck, T., Peterseil, J., Pröll, G., Geiger, S.: Providing high resolution data for the long-  
773 term ecosystem research infrastructure on the national and European scale, in:  
774 *Umweltinformationssysteme – Wie verändert die Digitalisierung unsere Gesellschaft?*, edited by:  
775 Freitag, U., Fuchs-Kittowski, F., Abecker, A., Hosenfeld, F., Springer Vieweg, Wiesbaden, 2021.

776 Working Group WRB: World Reference Base for Soil Resources 2014, update 2015 International soil  
777 classification system for naming soils and creating legends for soil maps, *World Soil Resources*  
778 *Reports No. 106*. FAO, Rome, 2015.

779 Wu, D., Ciais, P., Viovy, N., Knapp, A. K., Wilcox, K., Bahn, M., Smith, M. D., Vicca, S., Faticchi, S.,  
780 Zscheischler, J., He, Y., Li, X., Ito, A., ARNETH, A., Harper, A., Ukkola, A., Paschalis, A., Poulter, B.,  
781 Peng, C., Ricciuto, D., Reinthaler, D., Chen, G., Tian, H., Genet, H., Mao, J., Ingrisch, J., Nabel, J. E.  
782 S. M., Pongratz, J., Boysen, L. R., Kautz, M., Schmitt, M., Meir, P., Zhu, Q., Hasibeder, R., Sippel, S.,  
783 Dangal, S. R. S., Sitch, S., Shi, X., Wang, Y., Luo, Y., Liu, Y., and Piao, S.: Asymmetric responses of  
784 primary productivity to altered precipitation simulated by ecosystem models across three long-  
785 term grassland sites, *Biogeosciences*, 15, 3421–3437, <https://doi.org/10.5194/bg-15-3421-2018>,  
786 2018.

787 Yu, X., Orth, R., Reichstein, M., Bahn, M., Klosterhalfen, A., Knohl, A., Koebisch, F., Migliavacca, M.,  
788 Mund, M., Nelson, J. A., Stocker, B. D., Walther, S., and Bastos, A.: Contrasting drought legacy  
789 effects on gross primary productivity in a mixed versus pure beech forest, *Biogeosciences*, 19,  
790 4315–4329, <https://doi.org/10.5194/bg-19-4315-2022>, 2022.

791 Zweifel, R.: Radial stem variations - a source of tree physiological information not fully exploited yet,  
792 *Plant Cell and Environment*, 39, 231–232, <https://doi.org/10.1111/pce.12613>, 2016.

793 Zweifel, R., Pappas, C., Peters, R. L., Babst, F., Balanzategui, D., Basler, D., Bastos, A., Beloïu, M.,  
794 Buchmann, N., Bose, A. K., Braun, S., Damm, A., D’Odorico, P., Eitel, J. U., Etzold, S., Fonti, P.,  
795 Rouholahnejad Freund, E., Gessler, A., Haeni, M., Hoch, G., Kahmen, A., Körner, C., Krejza, J.,  
796 Krumm, F., Leuchner, M., Leuschner, C., Lukovic, M., Martínez-Vilalta, J., Matula, R., Meesenburg,  
797 H., Meir, P., Plichta, R., Poyatos, R., Rohner, B., Ruehr, N., Salomón, R. L., Scharnweber, T.,  
798 Schaub, M., Steger, D. N., Steppe, K., Still, C., Stojanović, M., Trotsiuk, V., Vitasse, Y., Arx, G. von,  
799 Wilmking, M., Zahnd, C., and Sterck, F.: Networking the forest infrastructure towards near real-  
800 time monitoring – A white paper, *Science of The Total Environment*, 872, 162167,  
801 <https://doi.org/10.1016/j.scitotenv.2023.162167>, 2023.

802 Zweifel, R., Etzold, S., Basler, D., Bischoff, R., Braun, S., Buchmann, N., Conedera, M., Fonti, P.,  
803 Gessler, A., Haeni, M., Hoch, G., Kahmen, A., Köchli, R., Maeder, M., Nievergelt, D., Peter, M.,  
804 Peters, R. L., Schaub, M., Trotsiuk, V., Walthert, L., Wilhelm, M., and Eugster, W.: TreeNet–The  
805 Biological Drought and Growth Indicator Network, *Front. For. Glob. Change*, 4,  
806 <https://doi.org/10.3389/ffgc.2021.776905>, 2021.

807